APPLICATION OF OPTICAL FIBERS FOR ROBOTIC TACTILE SENSING

by

Peng-Lung Terence Chen

Submitted in Partial Fulfillment of the Requirements for the Degree of Master of Science in the Electrical Engineering Program

Salvatore R. Pansino — 6/5/87

Advisor — **Date**

Sally M. Hotchkiss — June 5, 1987

Dean of the Graduate School — **Date**

YOUNGSTOWN STATE UNIVERSITY

JUNE, 1987

ABSTRACT

APPLICATION OF OPTICAL FIBERS FOR ROBOTIC TACTILE SENSING

Peng-Lung Terence Chen
Master of Science, Electrical Engineering
Youngstown State University, 1987

The use of optical fibers as contact pressure sensors is shown to be an effective means of providing tactile sensing for robots. An overview of optical fibers including their use as sensors is given. The attenuation of a light signal propagating in an optical fiber due to microbending of the fiber is investigated. The dependence of attenuation on the extent of microbending is explained using optical waveguide theory. Several designs of optical fiber tactile sensors for robots are described. The output signal is converted from analog to digital form by an Analog/Digital converter. A microcomputer is then used to process the signal from the sensor to provide control signals for the robot. The complete system is described including the design, construction, and test results.

ACKNOWLEDGEMENTS

I would like to express my sincere gratitude to Dr. Salvatore R. Pansino, chairman of the Electrical Engineering Department, for his continuous guidance and assistance in the preparation of this thesis.

I would like to thank Dr. John Berthold, Babcock & Wilcox Alliance Research Center, Dr. Duane F. Rost, Dr. M. Siman, and Dr. J. Jalali, Electrical Engineering Department. They provided me with valuable information and equipments for my experiment.

My deepest respect goes to my mother, who encouraged me to study in the U.S.A..

I would like to express my sincere thanks to Dr. Katz's family, who are my American host family. They provided me a warm home in Youngstown and helped me to adjust to my life in this country.

I would like to thank Mrs. Joy DeSalvo, instructor of the English Department, for her assistance with correcting my writing.

Finally, I would also like to thank Mr. Rich Laughlin, Engineering Technician, who gave me a generous amount of practical advice and valuable assistance.

TABLE OF CONTENTS

LIST OF SYMBOLS

SYMBOL	DEFINITION	REFERENCE
β , τ	Ray Invariants	EQ. 1
n	Refraction index	EQ. 1
ρ	Core Radius	EQ. 6
r	Bend Fiber Radius	FIG. 8
T	Transmission Coefficient	EQ. 16
z_p	Ray Half-period	EQ. 17
P	Light Power in Fibers	EQ. 18
θ_c	Complement of the Local Critical Angle	EQ. 21
e	Electronic Charge	EQ. 22
h	Plank's constant	EQ. 22
η	Quantum Efficiency	EQ. 22
S	Sensitivity of the Photodiode	P. 27
λ	Clamp wavelength	Fig. 11
B	Helix Width	Fig. 12
γ	Power Attenuation Coefficient	EQ. 18
ϕ_p	Angle between CP and CQ in Fig. 8	Fig. 8

LIST OF FIGURES

LIST OF FIGURES (Continued)

LIST OF TABLES

LIST OF TABLES

CHAPTER 1

INTRODUCTION

1.1 OBJECTIVE

The purpose of this thesis is to explore the application of fiber optic pressure sensors to provide tactile sensing for robots. In addition to and in support of the main objective, these are the following goals:

1. **Establish** the importance of sensors and the impact of their characteristics on the system design.
2. **Provide** a basic understanding of optical fibers and how they can be used as sensors.
3. **Determine** the characteristics of fiber optic pressure sensors that are critical in designing a tactile sensing system for robots.

1.2 BACKGROUND

Sensors are an important part in engineering applications. Both instrumentation and feedback control systems cannot function without measurement, and good measurement must have proper sensors in the system. Sensors, also called detectors, are defined as devices that detect, measure, or record physical phenomena changes in the environment. Usually, sensors convert one form of energy, or physical quantity, to another form of energy. For example,

photodetectors sense light energy and convert it to electrical energy.

In recent years, many new types of sensors have been specified, designed, manufactured, and used. As well as other sensors, optical fiber sensors have been designed, experimented and used in engineering applications. As will be introduced in this thesis, optical fibers used as contact pressure sensors are shown to be effective and practical.

Before applying sensors in the system, the designer must have appropriate considerations for the whole system due to the characteristics of the sensor. However, general considerations for the sensor of the system include:

1. What kind of physical quantity will be measured?
2. What is the transduction principle of the sensor?
3. What part in the sensor responds directly to the environment change(measurand)?
4. What is the special characteristic of the sensor?
5. What is the range of the measurand?

Followed by the general considerations for the sensor system ,as mentioned above, the considerations of the optical fiber sensor system for this thesis become:

1. Tactile pressures are measurands in the system.
2. Optical fibers are the sensors in the system.
3. The transduction principle of optical fiber sensors is that the intensities of tactile pressures are transduced to the attenuations of light energy in the fiber. By using a photodetector to detect the changes

of light power, which represent the changes of pressures, electrical voltage outputs from the photodetector respond directly to the changes of pressure on the fiber.

4. The ranges of measurand(pressure) depends upon the designs of fiber sensors, which will be introduced in chapter four.

1.3 APPROACH

To plan the structure of the thesis, several steps are made. First of all, since optical fiber sensors are the main concern, the operation and advantages of the optical fiber system must be studied. Secondly, mathematical foundations of the waveguide theory , which predicts the light power loss due to microbendings of the fiber, can support the practical performances of the system. The third area of concern is the relationship between the applied pressure on the fiber and the light power attenuation of the photodetector. The relationship should be established before the system is built. In addition, the performances of different sensor designs should be examined to improve the efficiency of the system. The final step, and perhaps the most important step, is to build the system which monitors the intensity of the pressure and controls the signals.

The strategy in the system is to use a microcomputer to monitor the pressure and process it. The choice between using hard-wired ICs or a microcomputer system depends upon

the cost or the desired flexibility of the system. Usually, the microcomputer becomes the better solution as the complexity of the system or the desired flexibility increases. To increase the effectiveness of the optical fiber sensor system in this design, a microcomputer is used for flexible programming and effective control of the system for the same reason.

The best way to prove the use and effectiveness of the optical fiber sensors is to demonstrate the successful application of those sensors. By using such optical fiber sensors for the robot's tactile sensing ability in the system, the expected results of this thesis becomes:

1. Optical fiber sensors are practical in detecting contact pressures.
2. Microcomputers are effective in monitoring the intensity of the pressure, and processing the information.
3. The robot will have tactile pressure sensing ability.

1.4 SYSTEM DESCRIPTION

Figure 1 shows the block diagram of the system design. The system includes several subsystems such as optical fiber sensor system, signal amplification system, Analog/digital conversion system, microcomputer, and robot system.

The microcomputer controls the operation of A/D conversion system and the robot. The fiber sensor, which is

built on the robot's hand, responds the contact pressure signals on the robot's hand. Then, these signals are sent to the computer through the A/D conversion system.

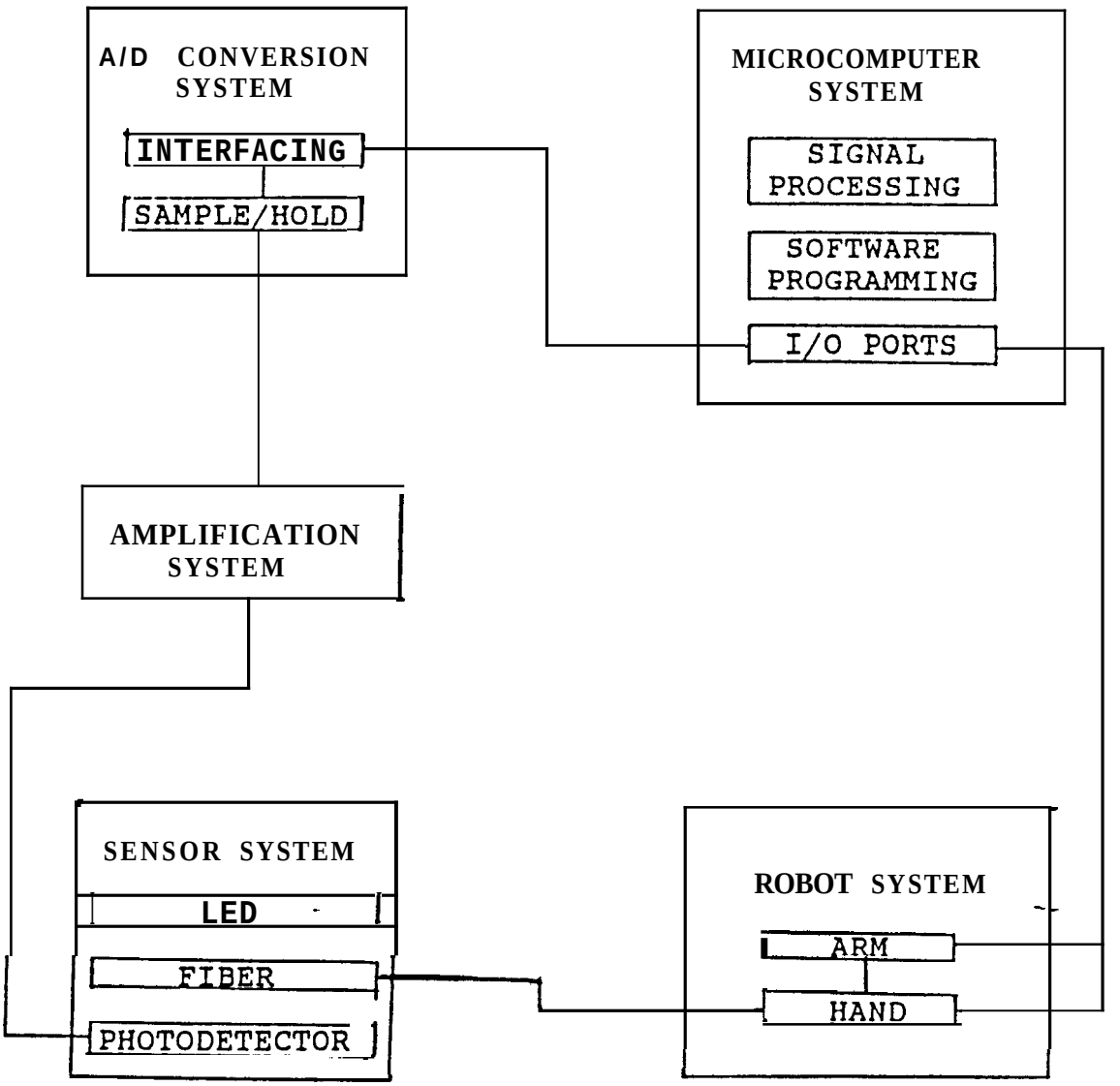

Fig. 1.--Block Diagram of the System.

The purpose of the A/D conversion system is to convert the analog voltage outputs from the sensor system to their digital forms for digital computer acceptance. Also since the signals from the sensor system are too small to measure directly, an amplification system is needed to amplify the signals.

Finally, the robot is also programmed and controlled by the microcomputer so that the microcomputer can monitor the whole system.

1.5 OVERVIEW

The overview of this thesis is based on the plan which was introduced in the last section. Chapter 2 will introduce the characteristics, basic principles, types, and advantages of optical fiber sensors. The chapter will also include optical fiber transmission systems and the introduction of optical fiber pressure sensors. Chapter 3 will discuss the waveguide analysis of the fiber's bendings with both ray and wave concepts. This approach predicts the behavior of light power attenuations due to microbendings of the fiber. Chapter 4 will give the experimental results of the relationship between applied pressures and light power attenuations. Sensor designs are also discussed in this chapter. Since the experimental data will be used to calibrate the sensor response in the software programming, the relationship of the sensor structure and the sensor response will be analyzed in that

chapter . Chapter 5 will deal with Analog/Digital conversion. Interfacing of the A/D converter and the microcomputer is also described. Since multi-input sensor systems are commonly used in sensor applications, the configuration of such sensor system is also discussed. In Chapter 6, matrix array configuration of the fiber sensor will be discussed. Such configuration of the fibers can be an effective method for robot's tactile sensing. Furthermore, the state-space approach will be used to approach the matrix configuration of the sensor system. Finally, the summary and the conclusion of this thesis will be presented in Chapter 7.

CHAPTER 2

OPTICAL FIBER SENSORS

2.1 INTRODUCTION

In recent years, scientists have tried to improve the methods of converting physical quantities into electric signals. In the development of optical fiber sensors, there is a superior way to detect environmental perturbation: converting physical parameters into light signals by fiber sensors, then converting light signals into electric signals.

More than 70 different types of optical fiber sensors have been developed and demonstrated. Because of fiber sensors[1] conspicuous properties, it is believed that the development of fiber sensors will keep on growing. These high sensitivity devices can measure wide ranges of physical parameters, such as temperature, pressure, acoustical energy, acceleration, etc. To lead to the analysis of such sensors, section 2.2 introduces the structure of transmission fibers. Secondly, the optical fiber transmission link is described in section 2.3 since fibers are useless without light sources and receivers. Then, the analysis of optical fiber sensors is carried out in section 2.4 , which includes the advantages, types, and characteristics of such sensors. Section 2.5 specifies the

basic operating principles, advantages, and limitations of optical fiber pressure sensors, since such sensors are the main concern of this thesis.

2.2 FIBERS

A typical fiber includes three parts: the core, the cladding, and the buffer coating. Although there are many different structures of the optical waveguide, the most accepted configuration of transmission fiber is a single solid dielectric cylinder ,which is the core of the fiber. As shown in Fig. 2, the core is surrounded by a dielectric cladding having a refractive index that is less than the refractive index of the core. According to Snell's law in Optics, those rays which have incident angles greater than the critical angle in the core of a fiber will reflect at the interface of the core and the cladding. This law provides the basic principle of light propagation in the fiber. In addition, the cladding reduces scattering loss due to the internal reflections of the light at the boundary of the core and the cladding. The elastic plastic buffer then encapsulates the fiber to prevent possible damage to the fiber.

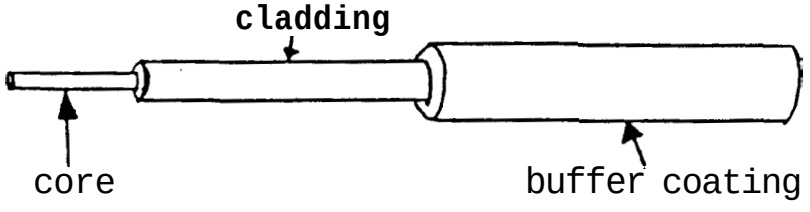

Fig. 2.--Structure of A Typical Fiber.

With different material compositions of the core, there are two commonly used fiber types: the step-index fibers, and the graded-index fibers. In step-index fibers, the refractive index of the core is uniform throughout the core and changes at the cladding boundary. For a graded-index fiber, the refractive index of the core is a function of radial distance from the center of the fiber.

Both the step-index and the graded-index fibers can be divided into single-mode and multimode classes. A single-mode fiber contains only one mode of propagation, whereas multimode fibers involve hundreds of modes. Multimode fibers offer several advantages compared to single-mode fibers. The larger core radii of multimode fibers make it easier to launch optical power into the fiber, and easier to faciliate the connection of similar fibers. Also in multimode fibers the optical power can be launched by light-emitting-diode (LED) sources, whereas single-mode fibers must be stimulated by laser diodes. However, multimode fibers also suffer from intermodal dispersion. When an optical pulse is launched into a multimode fiber, the optical power of the pulse is distributed over all of the modes. Since each of the modes travels at a slightly different velocity, the pulse spreads out in time as it travels along the fiber.

2.3 OPTICAL FIBER TRANSMISSION LINK

All optical fiber systems employ at least one light source, one light detector, and one fiber for both communication and sensing purposes. The light source is for injecting a continuous light signal into the fiber. The detector is for receiving the light signal which converts it into a useful electric output. Usually, a typical optical fiber transmission link consists of elements such as the transmitter, the fiber, and the receiver as shown in Fig. 3. A transmitter comprises a light source, either a LED or a laser diode, and drive circuitry. A receiver consists of a photodetector and amplification circuitry. Fibers connect receivers and transmitters as signal transmission lines. For long distance signal communication purposes, signal repeaters are needed to guarantee the purity of the transmission signals. However, repeaters are not used in this design because fibers are used as sensors but not transmission lines.

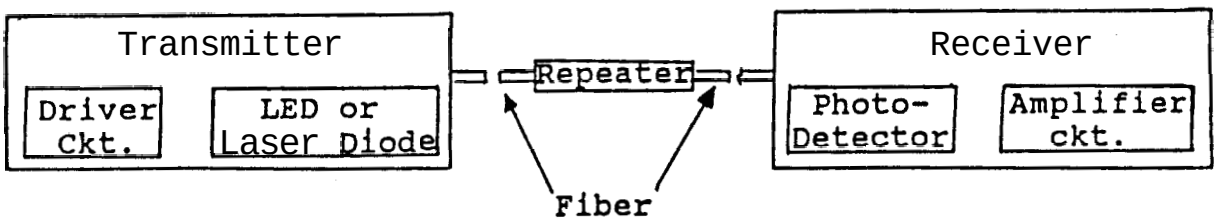

Fig. 3.--Optical Fiber Transmission Link.

The optical fiber transmission links, used in sensor systems, are basically the same as the links used in communication systems. The only difference is that some portions of the fiber in sensor systems have been designed as sensing elements. Depending upon the structure and the purpose, sensing elements will be stimulated by the particular environmental perturbation.

2.4 OPTICAL FIBER SENSORS

Optical fibers provide an outstanding method of sensing the changes of environmental parameters. Advantages of optical fiber sensors include small size, low cost, high efficiency, geometric versatility, and electromagnetic induction immunity. Because of the electromagnetic induction immunity, optical fiber sensor systems have lower noises than other sensor systems. Fiber sensors are the ideal sensors that can be used in high electrical noise environments since the light signal transmitted in the fiber will not be affected by electrical noises. Also because of their versability, optical fiber sensors can be suitable for many configurations and conditions. For example, fiber sensors can be designed with the length necessary for the specified application while it is difficult for other types of sensors to exceed a certain maximum length.

Generally, optical fiber sensors can be divided into extrinsic (phase, interferometric) type and intrinsic (amplitude) type. Extrinsic optical fiber sensors have a

broader range than intrinsic sensors. By using extrinsic sensors, light is processed out of the fiber by an external sensing element. Either light is reflected back into the transmission fiber, or a second fiber is used to recollect the modulated light. The external sensing element is either a mechanical structure or a material, which is sensitive to the environmental perturbation to be measured. For example, replace a section of the fiber cladding by a material that is sensitive to index of refraction, a temperature sensor set is then constructed. A temperature change will induce a phase shift in the propagating light of the fiber. By using a fiber interferometer, the phase change is measured . Then, the phase change can be represented as the temperature change.

Contrary to extrinsic fiber sensors, intrinsic optical fiber sensors contain the light totally within the fiber. The modulation of this type is made by varying the amplitude of light in the fiber rather than interference modulation in extrinsic type sensors. The physical perturbation interacts with the intrinsic fiber or some devices attached to the fiber to directly modulate the intensity of the light in the fiber. For example, the optical fiber pressure sensor, which is the topic of this thesis, is an intrinsic type fiber sensor.

Because lights are processed out of the fiber, extrinsic optical fiber sensors have disadvantages such as dirt affection, contamination, and mechanical vibration.

Contrary to extrinsic sensors, intrinsic sensors process light inside the fiber. The signal will not suffer from the bad environment. In some particular applications, fibers can be used in high temperature, high stress, or high nuclear radiation environment if they were coated with special material such as metal.

The advantages of intrinsic sensors are the simplicity of construction and the compatibility with multimode fiber technology. From the sensor system design point of view, extreme sensitivity is not required for most applications. As a result, these intrinsic fiber sensors are competitive with existing devices.

2.5 OPTICAL FIBER PRESSURE SENSORS

A wide range of fiber sensors can be characterized as intrinsic (amplitude) fiber sensors. Any transduction execution which provides a change in optical intensity proportional to an applied signal can be classfied as such a sensor. The contact pressure sensor used in this thesis is an intrinsic type of fiber sensors.

The amount of light loss in the optical fiber is sensitive to the curvature of the fiber. Optical fiber pressure sensors are based on utilizing this loss-change characteristic. Bending fiber at specific points along its length tends to disrupt internal reflections of the light. A certain portion of light paths, or transmission modes, escape out of the fiber core by those disruptions. Then,

some propagating modes of the fiber are changed to the radiation modes. When the fiber is bent in such a way that the distortion has wave numbers equal to the difference in wave number between the propagating and radiating mode, strong light loss occurs. The amounts of light intensity change after disruptions are then modulated to represent the intensity of the bending. Since bendings of the fiber are caused by the applied pressure on the fiber, optical fibers are utilized as contact pressure sensors.

The important advantage of the microbend contact pressure is that the optical signal is maintained within the fiber, which means such sensors can be used in harsh environments. In addition, the transduction mechanism of such sensors is compatible with multimode fibers. As mentioned in the second section of this chapter, multi-mode fibers can handle light signals weaker than single-mode fibers. Thus, weak signal detection is promising in the optical fiber contact pressure sensor system.

Finally, depending on the design, several methods can achieve the bending of the fiber, such as twisted fibers method and the microbending method. In this thesis, the microbending method is used. The detail and the experimental results will be analyzed in chapter 4.

CHAPTER 3

WAVEGUIDE ANALYSIS

3.1 INTRODUCTION

In this chapter, power attenuation due to bending of the fiber is studied by the optical waveguide theory. Ray analysis is used since the fiber, which is used as sensor, is a multimode type in the system. The radiation loss due to the bending of the fiber is described by leaky rays which are either refracting or tunneling. To lead to the power attenuation of the leaky rays, ray invariants are introduced in the second section of this chapter. The third section analyzes the light power loss due to the bending of the fiber.

3.2 RAY INVARIANTS

Snell's Law in Optics describes the relation between the refraction angle and the incident angle as light rays travel between two different refraction index materials. From Snell's Law, one can define the translational invariance of the waveguide.

As shown in Fig. 4, the ray invariant for the step-profile planar waveguide is expressed as:

$$\beta = n_{co}\cos\theta_z = n_{cl}\cos\theta_t. \qquad (1)$$

where n_{cl} , n_{co} are the refraction index of the core and

of the cladding respectively.

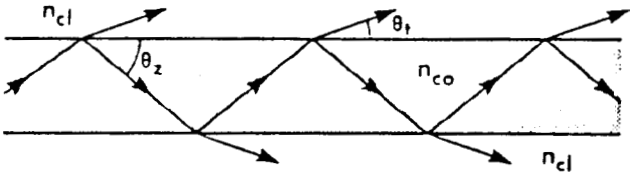

Fig. 4.--Light path of a step-profile planar waveguide.

The relationship between the ray invariant and the propagation direction classifies rays as bound rays and refracting rays. Bound rays satisfy the condition $n_{cl} < \bar{\beta} \leq n_{co}$, , whereas refracting rays satisfy the condition $0 \leq \bar{\beta} < n_{cl}$

The refraction index of the graded-profile planar waveguide is a function of the core radius. This causes the bound rays to propagate along a sinusoidal-like path in the core as shown in Fig. 5.

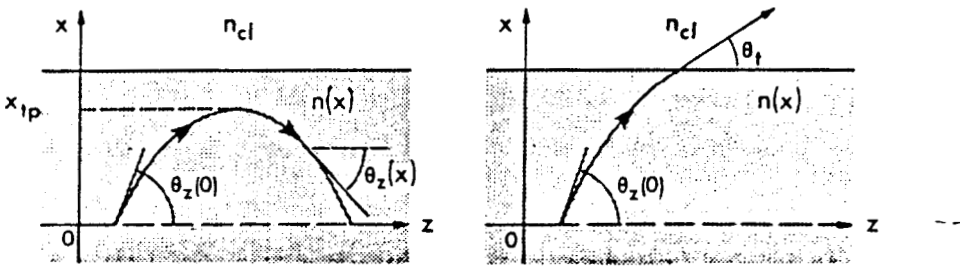

Fig. 5.--Ray paths of a graded-profile planar waveguide.

As the rays bend when they propagate in the core, these rays will reach the turning points at x_{tp} or they will reach the interface where they refract out of the core. The

classification of those bound rays and refracting rays is also described by ray invariants. Since the refraction index is a function of the core radius, the ray invariants for the graded-profile planar waveguide are defined as:

$$\bar{\beta} = n(x)\cos\theta_z(x) = n(x)\frac{dz}{ds}. \tag{2}$$

As $x = 0$ and $\theta_z(0) = \theta_c(0)$ in Eq. (2), bound rays satisfy the condition $n_{cl} < \bar{\beta} \leqslant n_{co}$, whereas refracting rays satisfy $0 \leqslant \bar{\beta} < n_{cl}$.

Optical fiber waveguides can transmit light signals over longer distances than planar waveguides. However, as far as ray tracing is concerned, the only difference between fibers (circular waveguides) and planar waveguides is the dimension, i.e. circular waveguides have three dimensional structures.

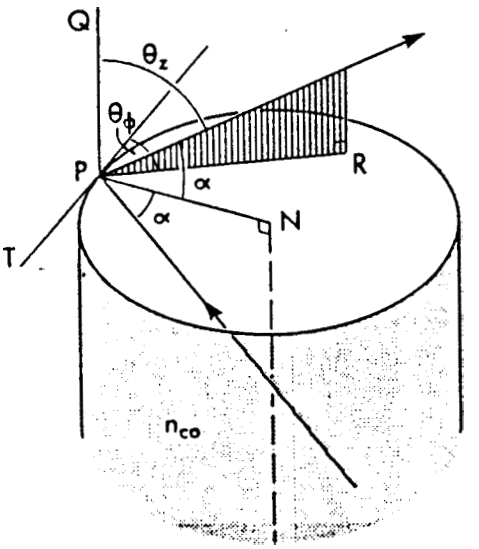

Fig. 6.--Ray path in a step-profile fiber.

According to Snell's Law, a ray will refract at P if $0 \leq \alpha < \alpha_c$ in Fig. 6, where a_c is the critical angle which is defined by

$$\sin a_c = n_{cl}/n_{co} = \cos\theta_c, \tag{3}$$

Also, for the rays that satisfy $0 \leq \theta_z < \theta_c$, they will be bound in the fiber. However, since the fiber has a three-dimension configuration, it represents a cone of angles at each position in the core cross-section, and includes both meridional and skew rays. The remaining skew-ray directions which are neither bound nor refracting rays belong to another class called tunneling rays. The tunneling rays satisfy the condition $\alpha_c \leq a \leq \pi/2$, and $\theta_c \leq \theta_z \leq \pi/2$ Both refracting and tunneling rays are known as leaky rays.

To analyze the ray invariant for the step-profile fiber, it is convenient to define two invariants in terms of the angles. If one defines the skewness angle according to the symmetry of the fiber, then the ray invariants become:

$$\begin{gathered} \bar{\beta} = n_{co}\cos\theta_z; \qquad \bar{l} = n_{co}\sin\theta_z\cos\theta_\phi, \\ \bar{\beta}^2 + \bar{l}^2 = n_{co}^2\sin^2\alpha, \end{gathered} \tag{4}$$

Therefore, the classification of rays in step-profile fibers becomes:

$$\begin{aligned} &\text{Bound rays:} && n_{cl} < \bar{\beta} \leq n_{co}, \\ &\text{Refracting rays:} && 0 \leq \bar{\beta}^2 + \bar{l}^2 < n_{cl}^2, \\ &\text{Tunneling rays:} && n_{cl}^2 < \bar{\beta}^2 + \bar{l}^2 \leq n_{co}^2 \quad \text{and} \quad 0 \leq \bar{\beta} < n_{cl}. \end{aligned} \tag{5}$$

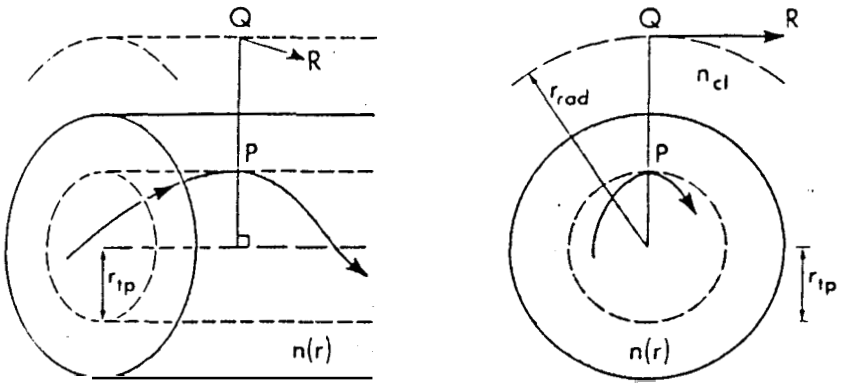

Fig. 7.--Ray path in a graded-profile fiber.

For graded-profile fibers (as shown in Fig. 7.) which has a refraction index that is a function of core radius, the ray invariants are:

$$\beta = n(r)\frac{dz}{ds} = n(r)\cos\theta_z(r), \qquad l = \frac{r^2}{\rho}n(r)\frac{d\phi}{ds} = \frac{r}{\rho}n(r)\sin\theta_z(r)\cos\theta_\phi(r), \tag{6}$$

and the classification of rays becomes:

$$\begin{aligned} &\textbf{Bound rays:} && n_{cl} < \beta \leq n_{co}, \\ &\textbf{Refracting rays:} && 0 \leq \beta^2 + l^2 < n_{cl}^2, \\ &\textbf{Tunneling rays:} && \beta_{min} \leq \beta < n_{cl} \quad \text{and} \quad n_{cl}^2 - \beta^2 \leq l^2 \leq l_{max}^2(\beta) \end{aligned} \tag{7}$$

where β_{min} and $l_{max}(\beta)$ for tunneling rays depend on the profile.

3.3 POWER LOSS OF THE BENT FIBER

For bent planar or circular waveguides, the light radiation loss is described by leaky rays which are either tunneling or refracting. Also, since the propagation of rays in a bent planar waveguide is identical to the propagation

of rays in the cross-section of a circular waveguide, and Fig. 8 can represent both cases.

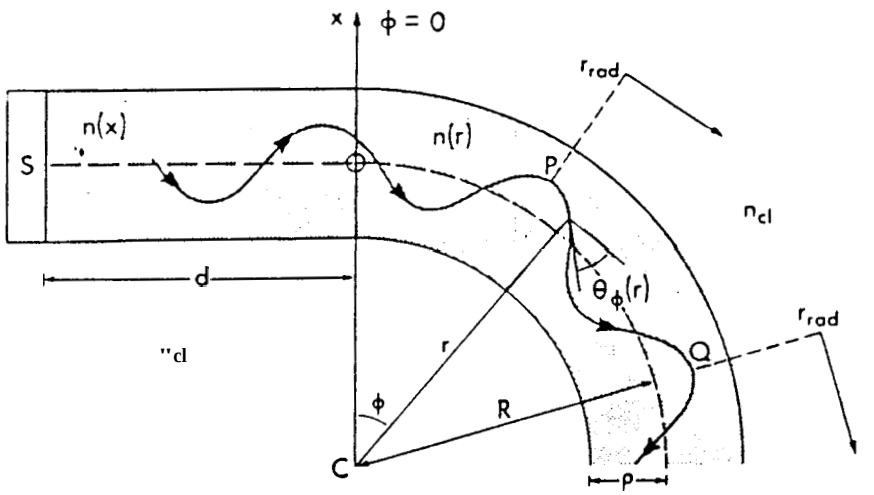

Fig. 8.--The cross-section of a bent waveguide.

As shown in Fig. 8, the cross-section of bent fiber has a curved section of radius R and a straight section of length d. A light source S illuminates the waveguide at Z=0. The distance d is considered sufficiently large compared with the curved section so that the light in the waveguide can reach the spatical steady state. In addition, the core profile shape n(r) is assumed unchanged by bending.

There are two interfaces between the core and the cladding. The symmetry of the bend guides every ray to follow a curved sinusoidal-like path. If the core is graded, then the light path has a shape as in Fig. 8, and if the core is a step-index core, then the light path has a zig-zag shape as in Fig. 9.

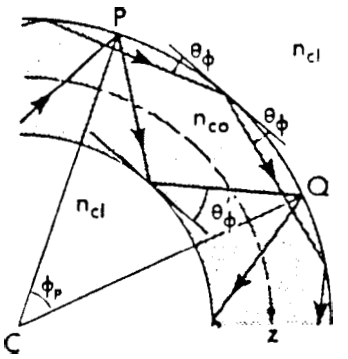

Fig. 9.--Ray paths on a bent step-profile waveguide.

To show that all rays in the bent section are leaky, the ray invariant for the bend has to be analyzed. The last section gave the definitions of the ray invariant for the waveguide theory. From Eq. (6), the ray invariant of the circular waveguide is:

$$T = \frac{r^2}{\rho} n(r) \frac{d\phi}{ds} = \frac{r}{\rho} n(r) \sin\theta_z(r) \cos\theta_\phi(r), \qquad \bar{\beta} = n(r)\frac{dz}{ds} = n(r)\cos\theta_z(r). \tag{8}$$

To find the radiation caustic on the bend, one should set $\theta_z(r) = \pi/2$ and define the bent ray invariant as

$$T_i = \{r/(R+\rho)\} n(r) \cos\theta_\phi(r), \tag{9}$$

where $R+\rho$ is the radius of the outer interface and is the angle between the tangent to the ray path and the azimuthal direction. At the beginning of the bend, $\theta_z(x) = \theta_\phi(r_0)$, where r_0 is the value of r at $\phi = 0$, so in the straight waveguide

$$\bar{\beta}_s = n(x)\cos\theta_z(x) = n(r_0)\cos\theta_\phi(r_0). \tag{10}$$

when $r = r_0$, the ray invariant becomes

$$T_b = \{r_0/(R+\rho)\}\,\bar{\beta}_s. \tag{11}$$

From Eq. (7), bound-ray invariants satisfy $n_{cl} < \bar{\beta}_s \leq n_{co}$, so the bent ray invariants are bourded by

$$n_{cl}(R-\rho)/(R+\rho) \leq \bar{T}_b \leq n_{co}, \tag{12}$$

since $\bar{T}_b$ must lie between $R+\rho$ and $R-\rho$

From Eq. (7), rays which satisfy the conditons

$$\bar{\beta} < n_{cl} \quad \text{and} \quad n_{cl}^2 < \bar{\beta}^2 + \bar{T}^2 \tag{13}$$

are called tunneling rays, since these rays appear to tunnel a finite distance into the cladding. For tunneling rays in the bend, the value of radiation caustic is given by

$$r_{rad} = \rho\bar{T}/(n_{cl}^2 - \bar{\beta}^2)^{1/2} \tag{14}$$

In the bend, since $\bar{\beta} = 0, \bar{T} = \bar{T}_b$ and ρ is replaced by $R+\rho$, then

$$r_{rad} = (R+\rho)\bar{T}_b/n_{cl}. \tag{15}$$

Since $\bar{T}_b$ is finite, the value of the radiation caustic is finite. Therefore, every ray in the bend is leaky. In addition, all rays are tunneling rays even in a slight bend.

Every ray in the bend radiates either by refraction or by tunneling. This radiation loss can by described by a transmission coefficient T. The definition of T is

$$T = 1 - \frac{\text{power in the reflected ray}}{\text{power in the incident ray}}. \tag{16}$$

Each ray loses a fraction of its power at each refraction. By summing the N transmission coefficients, then the power attenuation coefficient is defined by

$$\gamma = \frac{T}{z_p} = NT, \tag{17}$$

where z_p is a ray half-period.

The power in any position of the fiber distance Z with the initial power P(0) then becomes

$$P(z) = P(0)\exp(-\gamma z) \tag{18}$$

when the power attenuation coefficient γ is constant.

By replacing Z with the angular displacement , the power attenuation along the bend becomes

$$P(\phi) = P(0)\exp(-\gamma\phi) \tag{19}$$

where P(0) is the bound-ray power on the straight fiber. In Eq. (19), the power attenuation coefficient is

$$\gamma = T/\phi_p. \tag{20}$$

where ϕ_p is the angle between CP and CQ in Fig. 8.

The total ray power $P_s(\phi)$ at angle ϕ around the bend is determined by integrating Eq. (19) over the core cross-section and all ray directions. Thus,

$$P_s(\phi) = P(0)\int_{R-\rho}^{R+\rho} dr \int_{-\theta_c(r)}^{\theta_c(r)} \exp(-\gamma\phi)\, d\theta_z, \tag{21}$$

where $\theta_c(r)$ is the complement of the local critical angle referred to the center of curvature.

CHAPTER 4

SENSOR DESIGN AND EXPERIMENTS

4.1 INTRODUCTION

The purpose of this Chapter is to use the optical fiber as the transducing medium to sense an applied pressure. The characteristics of the receiver circuit which are important factors for sampling signals are discussed . Different types of sensors are used in the experiment to compare the signal distortions. The experimental results are analyzed in the last part of this chapter.

4.2 PHOTODETECTORS

The photodetector is a semiconductor device that converts optical signals into electric currents. In this experiment, a pin photodiode is used in a KOP-100 fiber optics kit (its circuit description and components characteristics are shown in Appendix A.). The pin photodiode is the most commonly used photodiode. Its depletion region thickness (the I layer) is adjusted to optimize the quantum efficiency and frequency response of the detector. The intrinsic (or I) layer of a pin photodiode is located between p- and n-type semiconductor material. The I layer supports a high electric field which causes

electron-hole pairs to separate quickly.

4.3 PRINCIPLE OF OPERATION

When a photodiode is illuminated by photons, electrons are pumped from the valence band into the conduction band. These electron-hole pairs are generated within the depletion region. Normally, a large reverse-bias voltage is applied across the photodiode. The resulting high electric field in the I layer causes the pairs to separate. These charge carriers are then collected across the reverse bias junction. If we ignore the recombination current loss in the depletion region, we can write the photocurrent as:

$$I = e\eta P/h \qquad (22)$$

where e, P, h, and η are the electronic charge, optical power, photon energy, and quantum efficiency respectively.

The output current from a photodetector is low. This means signal amplification and processing are required. A typical optical receiver, therefore, will contain a photodiode, an amplifer, and a filtering circuit.

As shown in Figure 10, a reverse-bias voltage is applied accross the pin photodiode. The current, which flows through the pin photodiode, is proportional to the incident optical power. This current is sampled by the resistor R allowing the photon flux to be measured as a voltage. By using this method, optical signals are transformed into electrical signals.

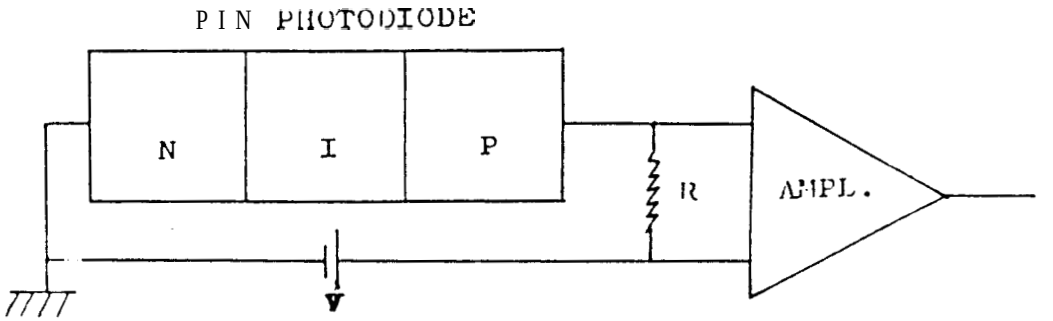

Fig. 10.--The pin photodiode receiver circuit.

Certain characteristics of photodetectors such as quantum efficiency, sensitivity, and linearity are important considerations in the system. Quantum efficiency is defined as the number of electron-hole pairs generated by each incident photon. Sensitivity (S) is defined as the current which is generated by the photodetector per watt of incident optical power (P), i.e., S=Current intensity/Light power. If the quantum efficiency is known, we can obtain the sensitivity from $S=\eta e/h\nu$, where h is Plank's constant, and ν is the light's frequency. The equation I=SP follows directly. The most important characteristic of a photodetector is linearity. The photocurrent varies linearly with the incident light power.

4.4 SENSOR DESIGN

The bending of the fiber at specific points along its length tends to disrupt the internal reflection. To analyze the relation between the applied pressure and the light intensity, we concentrate on the attenuation which is caused by the fiber distortion. To distort the fiber, several methods may be used such as the microbending method, the streched chain method, the twisted fibers method, and the spiral method. In this experiment, the spiral method , the microbending method, and the streched chain method are used.

4.4.1 MICRO-BEND SENSOR

Microbend sensors are constructed as shown in Figure 11. A wave shaped clamp is used to apply pressure to the fiber. A linear motion of amplitude A of the clamp imposes a distortion of the form $A\sin\lambda x$ on the fiber.

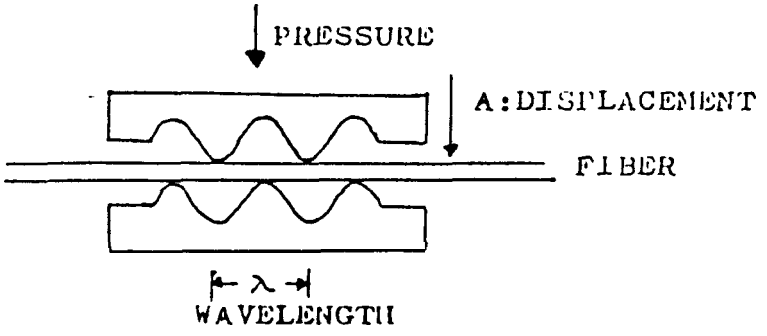

Fig. 11.--Microbend Sensor.

4.4.2 SPIRAL SENSOR

A spiral sensor is made by winding a wire around the optical fiber at the critical spiral pitch as shown in Figure 12. With a different helix width B or a different core radius of the winding wire, the fiber will respond to different types of distortions. The performance of the fiber distortion for different radius wires and different helix width is tested in this experiment.

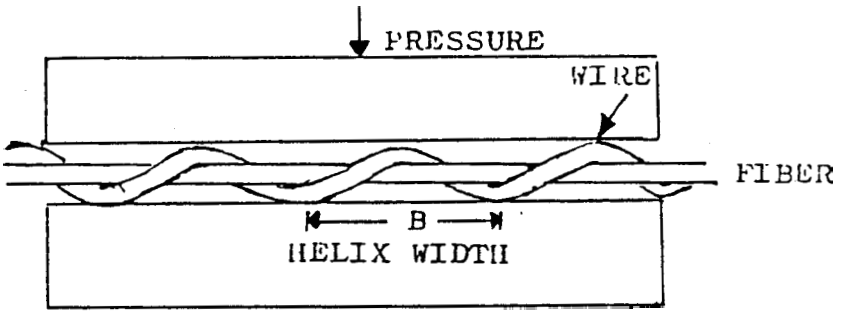

Fig. 12.--Spiral Sensor.

4.4.3 STRETCHED CHAIN SENSOR

Instead of the wave-shaped clamp of the microbend sensor, a roller chainlike device is used in this sensor as shown in Figure 13. The motion of the plates caused by an applied pressure at the top and bottom of the chain sensor forces the fiber to have a constant curvature distortion.

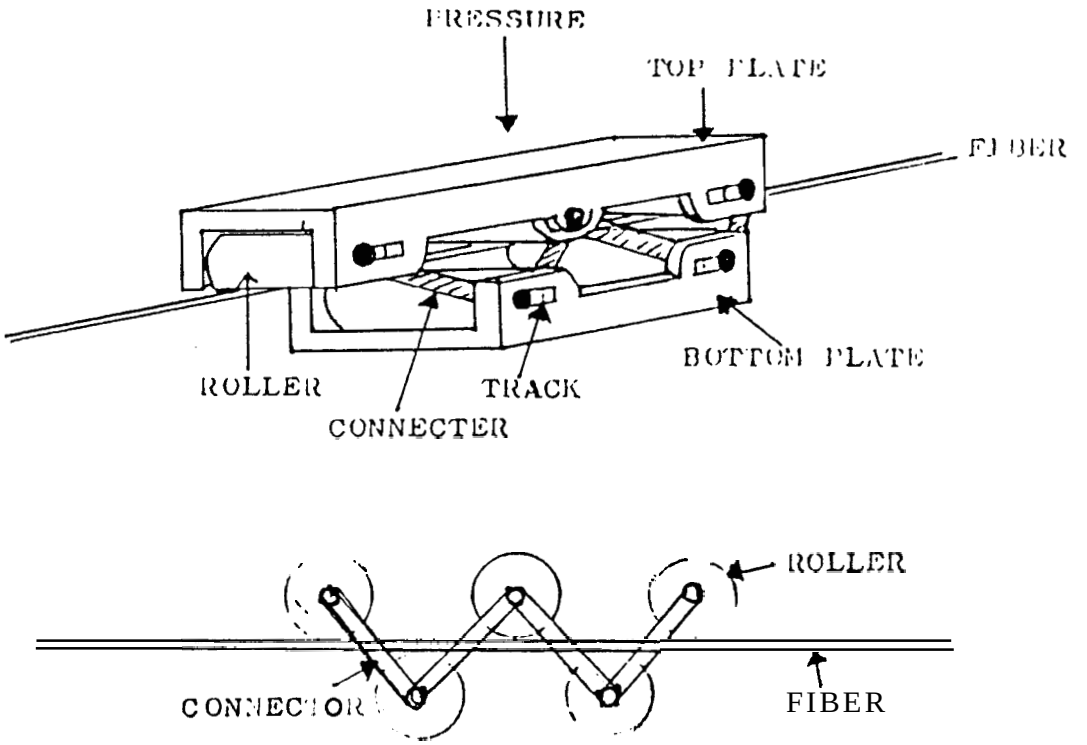

Fig. 13.--Stretched Chain Sensor.

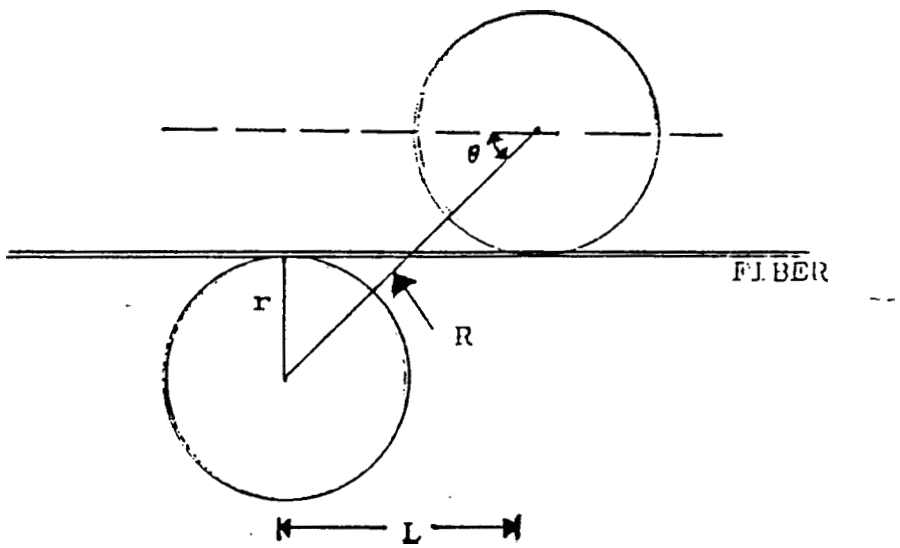

Fig. 14.--Geometric Diagram Of The Stretched Chain Sensor.

If the light loss per unit arc length is constant, the form of the loss vs displacement function of the sensor can be determined from the geometric diagram shown in Figure 14. The angle θ is defined as the angle between the horizontal axis and the roller connector. This angle will tend to zero as the sensor is fully stretched, and it will reach a maximum value: $\arcsin(2r/R)$, (where R is the length of the connector, r is the radius of the roller, and the diameter of the fiber is considered small compared to the diameter of the roller).

The fiber is tangent to the rollers when the sensor is not stretched. As the sensor is stretched, the change in contact arc length C with extension L becomes:

$$dC/dL=(dC/d\theta)/(d\theta/dL).$$

Since $(dC/d\theta)=-2r$, and $(d\theta/dL)=-R\sin\theta$, we derive:

$$dC/dL=2r/R\sin\theta \qquad (23)$$

Thus, the light transmission vs the displacement function needed to calibrate the sensor system is:

$$dT/dL=N(dT/dC)(dC/dL)$$

$$=N(\text{Constant})(2r/R\sin\theta) \qquad (24)$$

The value of dT/dC is a constant because it is assumed that the light loss per unit arc length is constant, and N is the number of rollers.

4.5 EXPERIMENTAL METHOD

For measuring the relation between the applied pressure and the light power attenuation in the fiber, the model shown in Figure 15 can be used. Consider an infinitesimal length dx of the fiber, the incident optical power P(x) attenuates dP as light propagates with the distance dx. Then, equation dp/dx=-aP(x) expresses the attenuation of the optical power, where a is the attenuation coefficient. As the light propagates L distance, the optical power becomes P(L)=P(0)e(-aL), i.e.

$$\log P(L)=\log P(0)-0.434aL.$$

Since the voltage output of the KOP-100's PREAMP is proportional to the optical power incident on the pin diode, so

$$\log(V(L1)/V(L2))=0.434a(L2-L1) \quad (25)$$

which also means $a=\log(V(L1)/V(L2)) / 0.434(L1-L2)$, where V(L1),V(L2) are the amplitudes of the signal corresponding to lengths L1, L2. By specifying the linear attenuation A in dB/m, the equation A(dB/m)=4.43a can be derived.

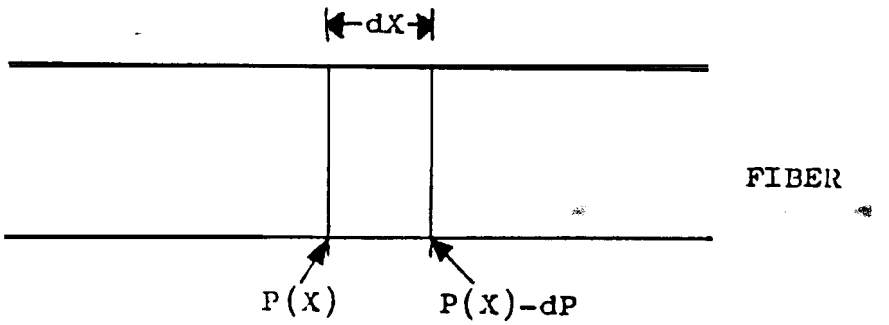

Fig. 15.--Model Of Light Power Propagation.

The output voltages of the KOP-100 vary with the loads applied to the sensor. Since the pressure is defined as force per area, the load over a given area will determine the magnitude of the pressure which is modulated by the output voltage attenuation.

4.6 EXPERIMENTAL DATA

The results of this experiment are based on the POCATEC model KOP-100 kit for light transmission and amplification, and SATEC model UTC-60HVL for the load testing.

4.6.1 TEST 1-DIRECT LOAD ON THE FIBER

SPECIFICATION: (1) Direct load on the fiber.

(2) Fiber diameter: 0.055inch.

(3) Load surface area: 3.72 square-inch.

TABLE 1

LOAD VS VOLTAGE ATTENUATION(Va) OF TEST 1

Load(lb.)	Va(mV)
5.0	0
10.5	1
14.7	2
20.3	3
25.0	4
29.7	5

4.6.2 TEST 2-MICRO-BEND SENSOR

SPECFICATION: (1) Fiber diameter: 0.055inch.

(2) Load surface area: 4.72 square-inch.

(3) Wave length of the clamp: 1.32 inch.

(4) Amplitude of the wave: 0.39 inch.

TABLE 2

LOAD VS VA OF MICRO-BEND SENSOR

Load(lb.)	Va(mV)	Load(lb.)	Va(mV)
0.2	0	4.5	113
0.5	3	5.0	130
1.0	7	5.5	155
1.5	12	6.0	194
2.0	21	6.5	216
2.5	31	7.0	249
3.0	44	7.5	275
3.5	58	8.0	312
4.0	80		

4.6.3 TEST 3-SPIRAL SENSOR (1)

SPECIFICATION: (1) Load surface area: 3.72 square-inch.

(2) Wire diameter: 0.022 inch.

TABLE 3

LOAD VS Va (B=0.5INCH) OF TEST 3

Load(lb.)	Va(mV)	Load(lb.)	Va(mV)
2.0	0	7.3	8
3.1	1	8.3	11
4.3	2	9.3	15
5.0	3	10.2	20
6.1	5		

TABLE 4

LOAD VS Va (B=0.78INCH) OF TEST 3

Load(lb.)	Va(mV)	Load(lb.)	Va(mV)
1.0	1	10.1	33
1.5	3	11.1	35
3.1	6	12.5	37
4.0	10	13.2	38
5.2	14	14.5	41
6.1	18	15.2	43
7.1	24	16.0	45
8.1	27	17.4	48
9.1	31		

TABLE **5**

LOAD VS VA **(B=1.18INCH) OF TEST 3**

Load(lb.)	Va(mV)	Load(lb.)	Va(mV)
1.0	1	11.3	15
2.1	3	13.5	16
3.5	5	15.2	18
4.6	6	16.3	19
5.8	8	18.2	23
6.4	9	20.6	25
7.5	10	22.6	26
9.7	12		

4.6.4 TEST 4-SPIRAL SENSOR (2)

SPECIFICATION: (1) Fiber diameter: 0.055 inch.

(2) Load surface area: 3.72 square-inch.

(3) Wire diameter: D=0,035 inch.

TABLE 6

LOAD VS Va (B=1.18INCH) OF TEST 4

Load(lb.)	Va(mV)	load(lb.)	Va(mV)
0.5	2	7.0	31
1.0	4	7.6	34
1.5	6	8.0	37
2.0	8	8.7	41
2.5	11	9.0	44
3.1	14	9.6	48
3.5	16	10.0	50
4.0	18	10.8	53
4.5	20	12.1	55
5.0	22	13.1	57
5.6		14.4	59
6.0	25	15.2	60
6.5	29	17.3	63

TABLE 7

LOAD VS Va (B=0.65INCH) OF TEST 4

Load(lb.)	Va(mV)	Load(lb.)	Va(mV)
1.1	0	10.8	9
2.5	1	12.1	11
3.7	2	13.2	12
5.1	3	14.4	13
6.1	4	15.7	15
7.1	5	16.7	16
8.3	6	17.3	17
9.6	8	18.2	19

4.6.5 TEST 5-STRETCHED CHAIN SENSOR

SPECIFICATION: (1) Load surface area: 1.90 square-inch.

(2) Roller diameter: 0.39 inch.

(3) Number of rollers: 5.

TABLE 8

LOAD VS Va OF STRETCHED CHAIN SENSOR

Load(lb.)	Va(mV)	Load(lb.)	Va(mV)
0.4	0	6.8	31
0.6	1	7.0	32
0.8	2	7.2	33
1.0	2	7.4	34
1.2	3	7.6	35
1.4	4	7.8	36
1.6	5	8.0	37
1.8	5	8.2	39
2.0	7	8.4	39
2.2	8	8.6	40
2.4	9	8.8	42
2.6	9	9.0	44
2.8	11	9.2	46
3.0	12	9.4	47
3.2	12	9.6	49
3.4	14	9.8	52
3.6	15	10.0	55
3.8	15	10.2	59
4.0	17	10.4	63
4.2	18	10.6	65
4.4	19	10.8	69
4.6	21	11.0	74
4.8	22	11.2	79
5.0	22	11.4	85
5.2	23	11.6	92
5.4	24	11.8	100
5.6	26	12.0	108
5.8	26	12.2	116
6.0	27	12.4	124
6.2	29	12.6	132
6.4	29	12.8	140
6.6	30		

4.7 ANALYSIS

Because of the material characteristic of the specific fiber used in this experiment, all results of the experiment indicate that there is a cut in pressure load. This cut in signal attenuation has a different value for each of the different methods of distorting the fiber.

The voltage attenuation(Va), which is modulated for the light power transmission loss, of test 1 increases approximately linearly as weight load increases. Since the weight is directly loaded on the fiber without spiral wire, the linearity of the signal output vs the pressure is good. However, the sensitivity of the pressure is not high enough for the sensor system. As shown in Figure 16, the cut in pressure load of the specific fiber is about 5 pounds over 3.72 square-inch surface.

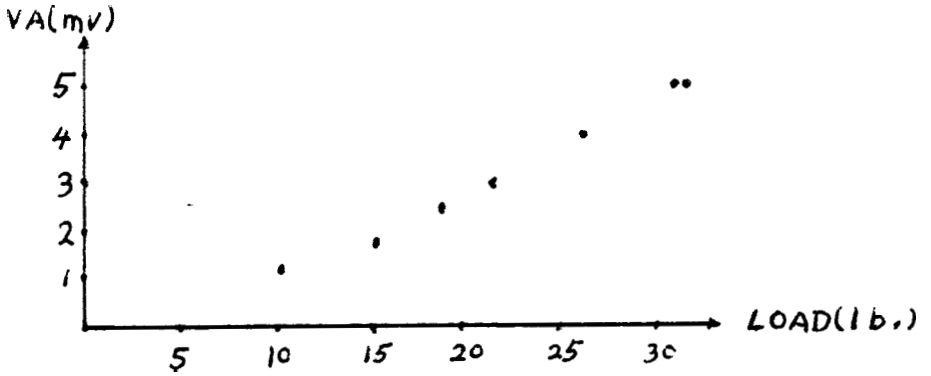

Fig. 16.--Load VS Va OF TEST 1.

In test 2, the micro-bend sensor is very sensitive to the applied pressure due to the amplitude and the helix length. With the load range from zero to eight pounds, the voltage attenuation increases from zero to 312mV. As shown in Figure 17, the shape of the voltage-load curve increases significantly when the load increases over 2.5 pounds. After 2.5 pounds, the voltage increases approximately linearly with the load.

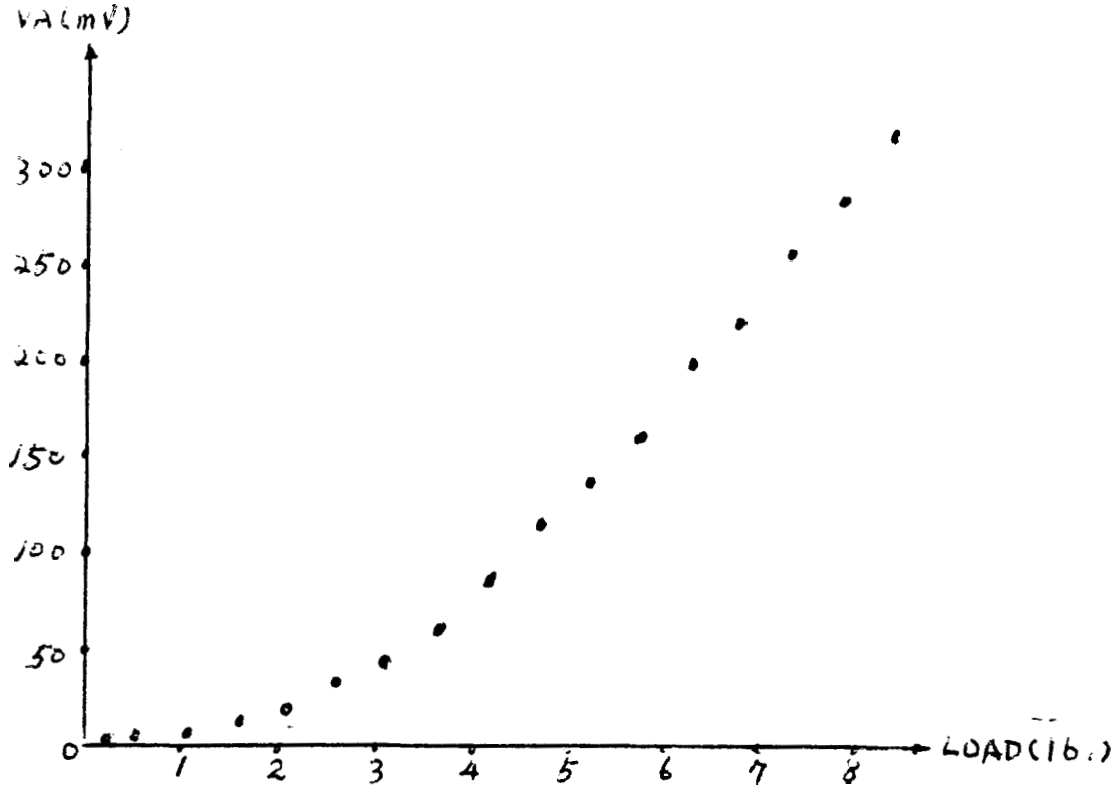

Fig. 17.--Load VS Va OF MICRO-BEND SENSOR.

The helix width B of the micro-bend sensor determines the number of bendings. The more bendings on the fiber, the more sensitive is the sensor to the applied pressure.

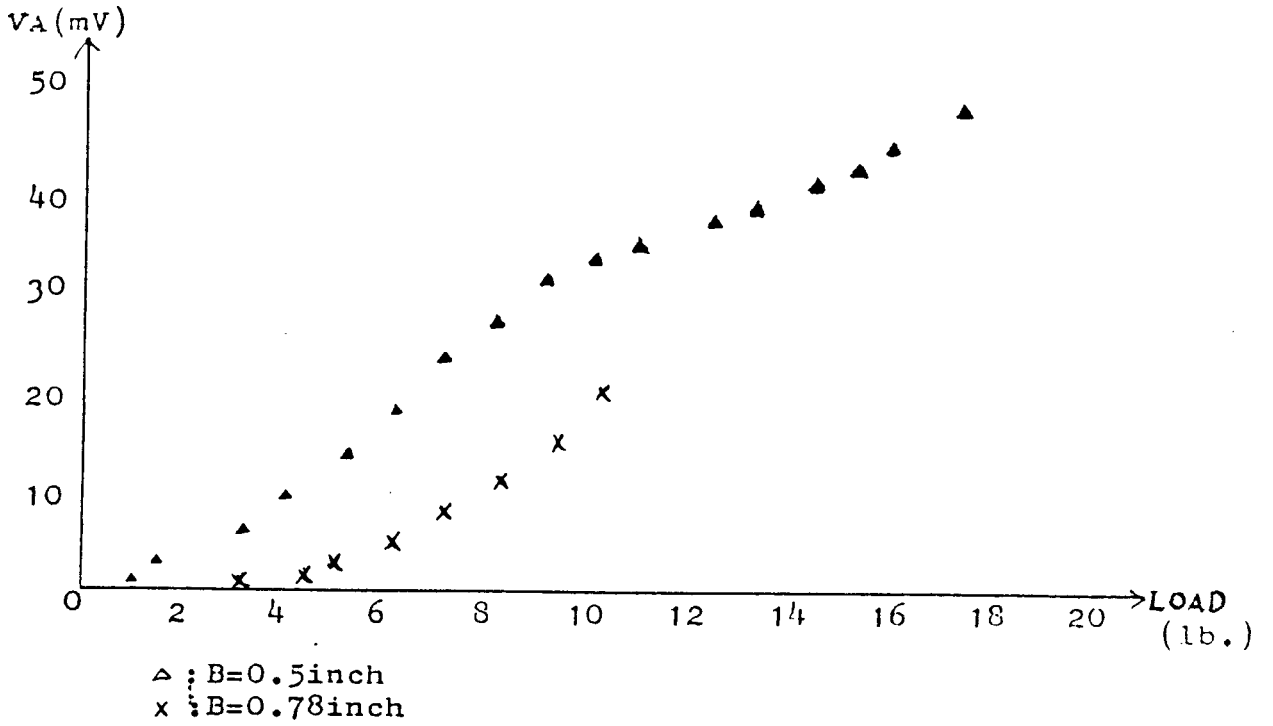

Fig. 18.--Load VS Va *of* test3.

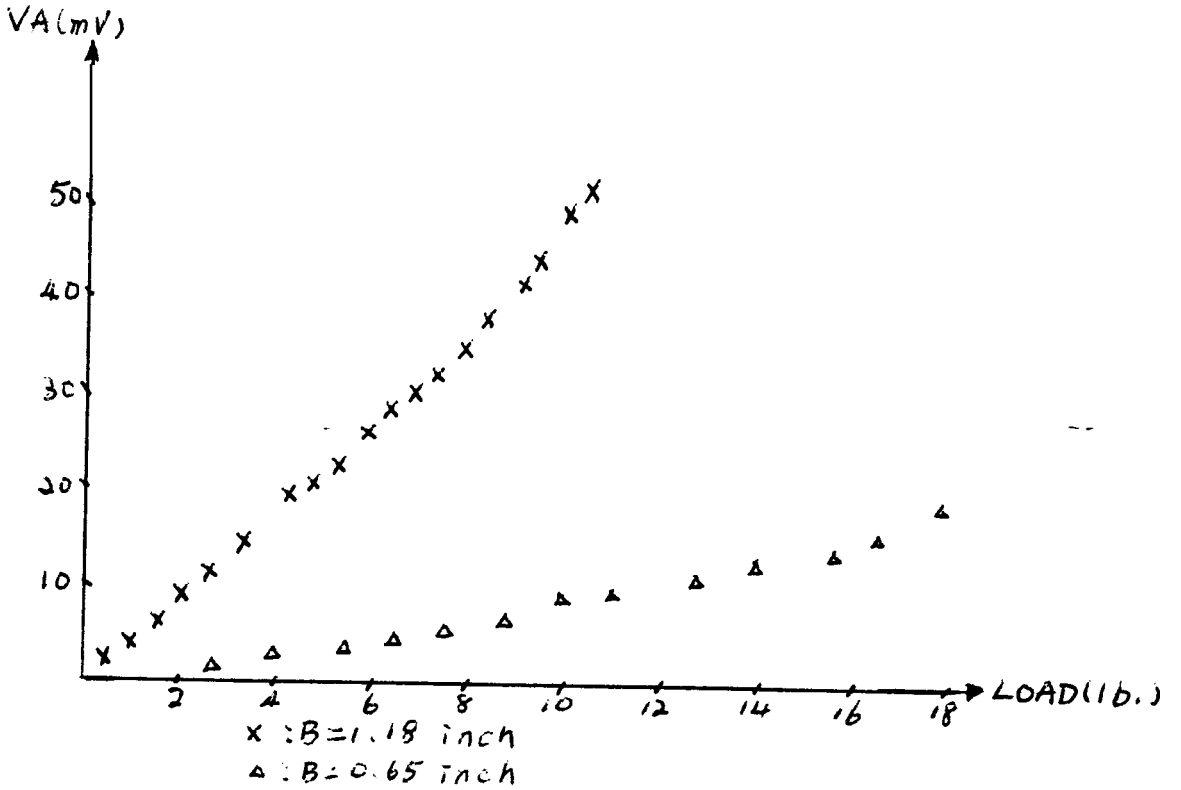

Fig. 19.--Load VS Va OF TEST4.

Figure 18 and Figure 19 show the results of test 3 and test 4. In test 4, the sensor exhibited a good linearity due to the diameter of the wire. The helix width determines the number of bendings on the fiber. A small helix width sensor has a higher sensitivity. However, test 3 indicates that the helix width B under certain value will make sensor output be nonlinear due to the deformation of the fiber.

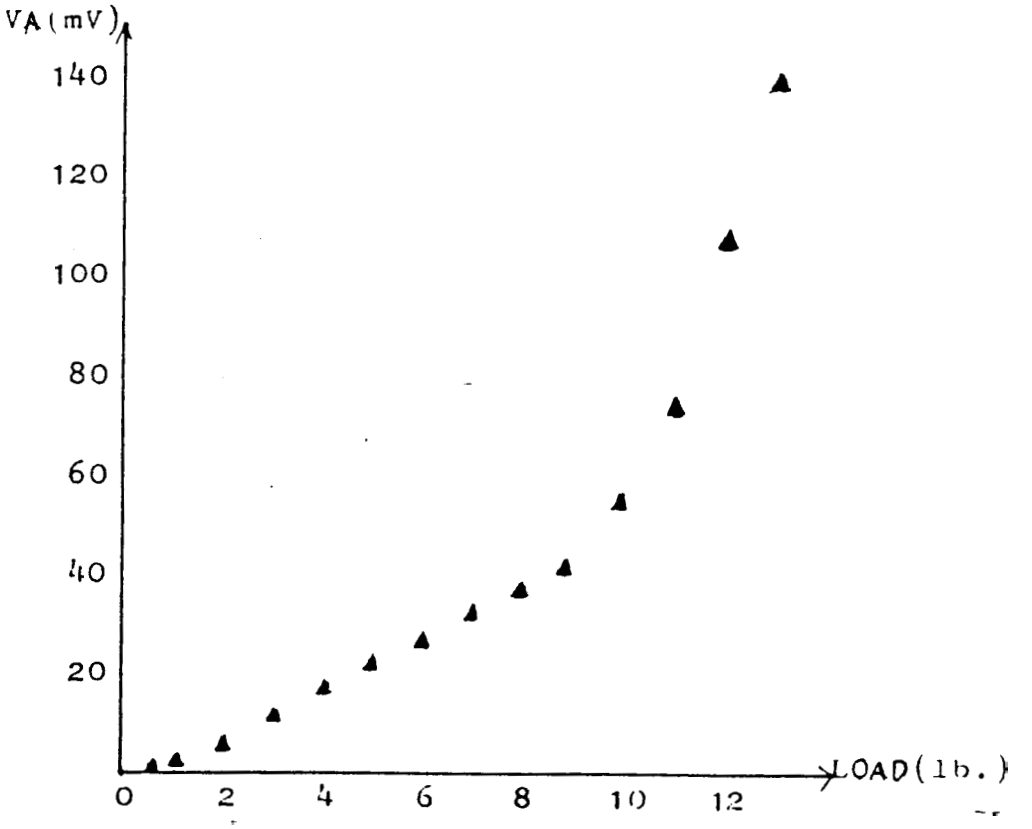

Fig. 20.--Load VS Va Of Stretched Chain Sensor.

The last test of the experiment is the stretched chain sensor. The experimental result shows an approximately linear property for loads under nine pounds. For the loads over nine pounds, signal attenuation increases rapidly due

to the plastic property of the fiber material. For the same reason as the case of the spiral sensor, the linear range of the sensor can be used for the tactile pressure detection.

4.8 SUMMARY

The approach for the sensor design has considerable latitude. Several methods can be used. However, the general considerations to obtain sensor design and linearity include:

(1) The diameter of the fiber.

(2) The surface area of the applied pressure.

(3) The number of bendings, and amplitude of the wave for the micro-bend sensor.

(4) The material properties of the fiber.

(5) The diameter of the winding wire, and the helix width for the spiral sensor.

(6) The radius of rollers, the connecter length, and the number of links of the stretched chain sensor.

In this chapter, several sensor designs to achieve fiber distortion have been tested and analyzed. Experimental results indicate that the optical fiber sensors for tacile pressure detection are effective and practical.

CHAPTER 5

DATA ACQUISITION

5.1 INTRODUCTION

Traditionally, sensors convert environmental variables into electric signals such as voltages and currents. As digital computers are used in sensor systems to monitor and processor these signals, it is necessary to convert these analog signals into their digital formats. For this Analog/Digital conversion purpose, a data acquisition system is used to interface the sensor and the computer. Usually, a data acquisition system includes an amplification circuit, a sample-hold circuit, a multiplexer, and an Analog/Digital converter. These interface systems and their components must be considered for good functionality, low cost, and high efficiency to meet the specific requirement. An interface system includes software and hardware, where software controls the operation of the system and gives the successive instructions for the hardware.

Sometimes in a sensor system, it is desired that the system has multiple-input channels. In other words, there may be several different sensors in the system. For example, if the system needs to monitor temperature and pressure changes of the environment at the same time, then the system must have multiple-input capability. To achieve this

purpose, the A/D converter coupled with a multiplexer can do the work. One convenient way to digitize datas from several sensors is to use the time-sharing process, i.e., the computer monitors those sensors in sequence.

5.2 ANALOG/DIGITAL CONVERSION

As mentioned above, most analog signals coming from sensors are either electric voltages or currents. If these signals are too small to be measured directly, then an amplification circuit must be used to match the A/D converter input range. Usually, the full scale input range of the converter may be 5V, 10V, or 25V.

There are several different types of A/D converters, and each type has different characteristics which depend on the specific system application. For computer interfacing, the successive approximation type converter has been in wide use because of its high speed of conversion which is in the MHz range and its high resolution.

The successive approximation techniques in an A/D converter consist of comparing the internal reference voltages with the unknown analog input voltage. Firstly, the most significant bit (MSB) is assigned to a logic 1 (high voltage level, 5V) if the analog input voltage is greater than the voltage from the comparator, and MSB bit is assigned to a logic 0 (low voltage level, ground) if the input voltage is less than the voltage of the comparator. Then the next most significant bit is compared. After the

least significant bit (LSB) is compared, the conversion is completed. During the conversion, the EOC (end of conversion) pin of the A/D converter will output a logic 0 to indicate the processing of the conversion, where an logic 1 on the EOC pin indicates that the conversion is completed. In addition, the analog input voltage should not be changed to acquire accurate digital outputs. To guarantee this, a sample-hold circuit can be added to the input of the system.

If a multiplexer is used in the data acquisition system, then this multiplexer must be addressed by the computer. For example, an 3-bit address decoder can decode the address fron the computer and decide which one of the eight channels is the input channel. Table 9 shows the relation of the address and the assigned channel. If the input address is set to all zeros from the computer, then channel "0" will be the analog input channel.

TABLE 9

ADDRESS AND ASSIGNED CHANNEL OF A 8-BIT MULTIPLEXER

Channel	Address code
0	0 0 0
1	0 0 1
2	0 1 0
3	0 1 1
4	1 0 0
5	1 0 1
6	1 1 0
7	1 1 1

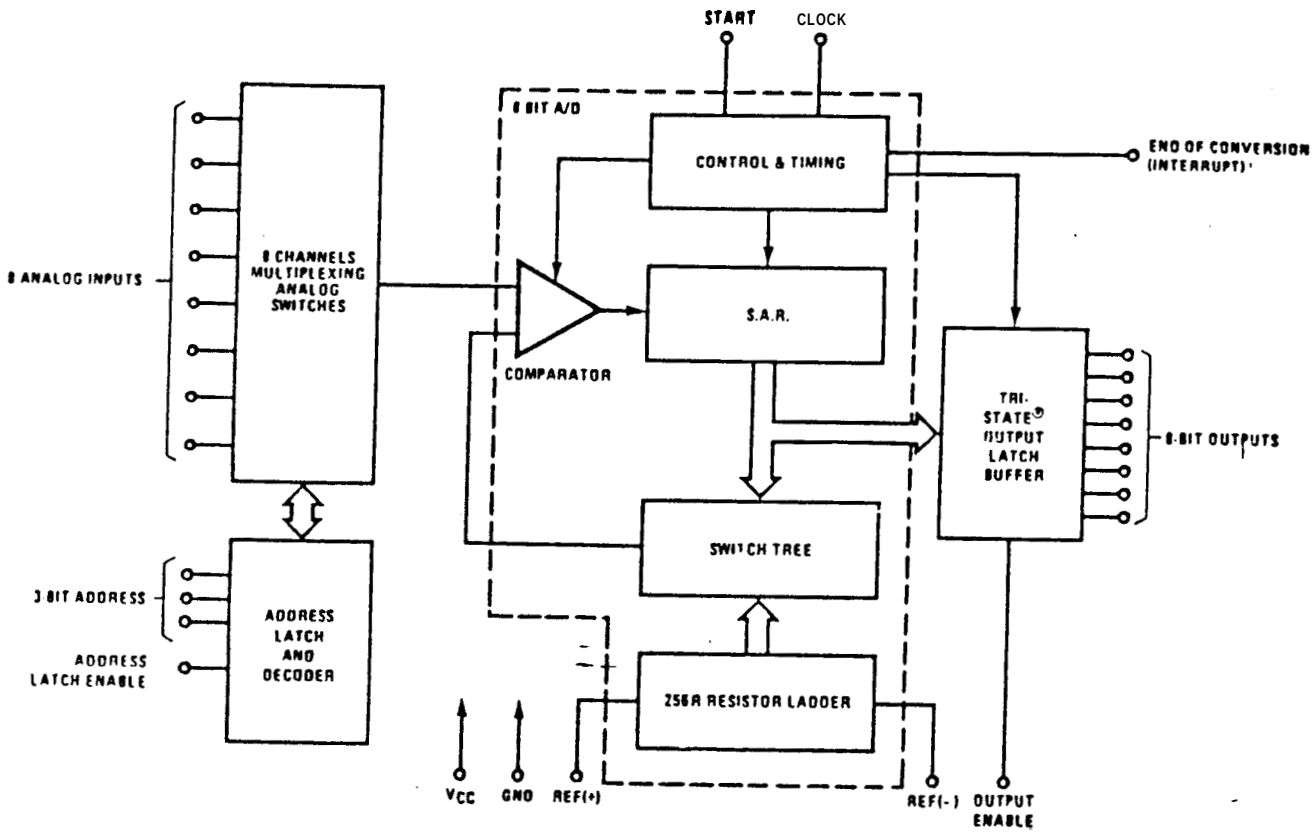

Fig. 21.--Block Diagram of an ADC0808.

5.3 SYSTEM DESCRIPTION

In this thesis, an ADC0808 data acquisition component is used. The ADC0808 is a monolithic CMOS device with an 8-bit A/D converter, an 8-channel multiplexer, and a microprocessor compatible logic. The 8-bit A/D converter uses successive approximation as the conversion technique.

The converter has a high impedance stablized comparator, a 256R voltage divider with analog switch tree, and a successive approximation register. The 8-channel input multiplexer can access any one of 8-single-ended analog inputs. As indicated in Fig. 21, the block diagram of the ASC0808, an external clock must be added since there is no internal clock to trigger the operation. Since there is only an optical fiber sensor used in the thesis, it is convenient to ground all 3-bit address pins of the multiplexer and use the channel o as the input pin.

After the channel of the multiplexer is assigned, the next step is to start the analog to digital conversion. When the START pin of the converter goes to a logical 1, the MSB data latch is set to a logic 1 and all other data latches are set to logic 0. As the START pin returns to low, the conversion sequence begins. After the START pin drops to logic 0, the microprocessor should check the EOC pin before entering the data into the computer.

In this thesis, an Intel SDK-85 is used to test the A/D conversion. Also, the high voltage level is assigned to 5V and the low voltage level is assigned to ground (OV). In addition, all ground points of the circuit should have a common ground for both analog and digital. Fig. 22 shows the interfacing of the ADC0808 and the Intel SDK-85 of the system.

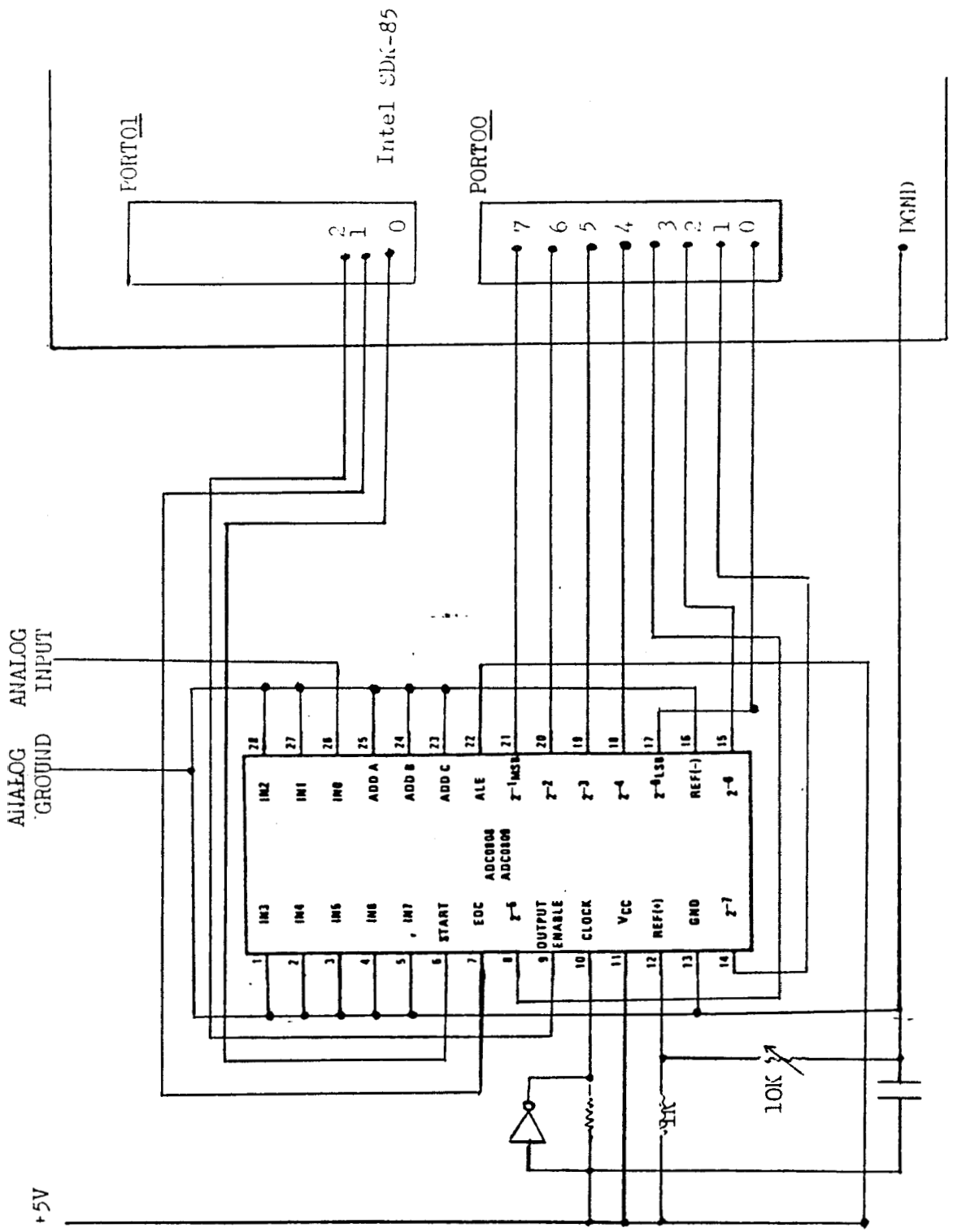

Fig. 22.--Interfacing Of An Intel SDK-85 And An ADC0808.

The external clock frequency is designed to 6 MHz since this value is the typical frequency for the ADC0808. The REF(-) pin of the ADC0808 is grounded because the unipolar operation is used in the system , and the analog input pin (AIN) is designed to have the input range from OV to 5V. The reference voltage is adjusted by the potentiometer of the circuit to acquire the accurate 5V full scale. To achieve this, one should set the analog input at 5V and continue the conversion by the Intel SDK-85. Then, adjust the potentiometer until the LSB bit output is flashing between logic 1 and logic 0.

To handshake the ADC0808 and the Intel SDK-85, the flow chart in Fig. 23 follows the steps which are discussed above. The assembler program for the SDK-85 is written as follows:

```
     SOURCE STATEMENT          COMMENT

       MVI A,05          *ASSIGN BITS 0,2 OF PORT 01 AS
       OUT 03                   OUTPUT BITS
       MVI A,01          *SEND A PULSE TO START PIN
       OUT 01                   THROUGH PIN 0 OF PORT01
       MVI A,00
       OUT 01
       MVI A,02          *ASSIGN BIT 1 OF PORT 01 IS--
       IN  03                   INPUT
       MVI A,00          *CLEAR ACCUMULATOR
LOOP1: IN  01            *CHECK EOC PIN OF ADC0808
       CPI 00            *COMPARE [A] WITH "00"
       JZ  LOOP1         *IF CONVERSION IS NOT COMPLETE
                                JUMP TO LOOP1
       JMP LOOP2         *IF CONVERSION IS COMPLETE
                                JUMP TO LOOP2
LOOP2: MVI A,FF          *ASSIGN PORT 02 ALL INPUT
       IN  02
       IN  00            *INPUT 8-BIT DATA FROM ADC0808
```

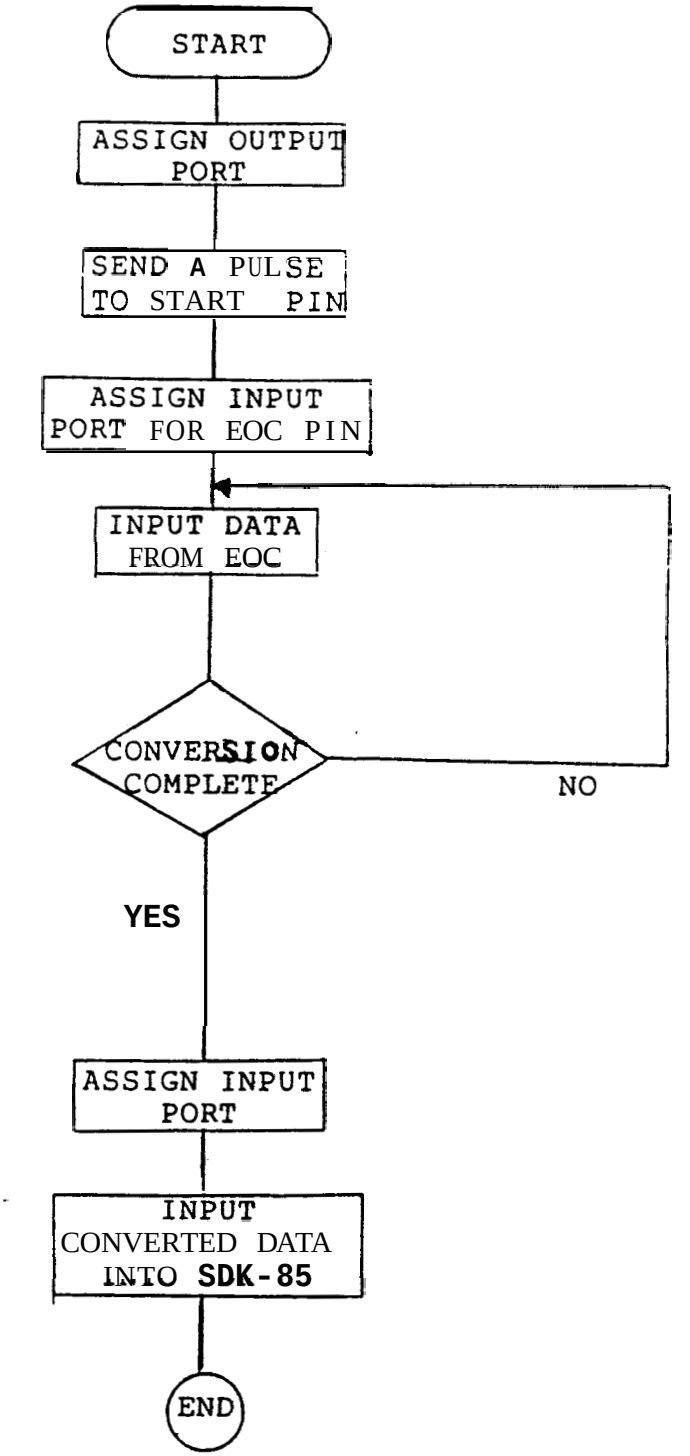

Fig. **23.--Flow** Chart Of Handshaking.

5.4 SUMMARY

Computer-controlled sensor systems have evolved to the configuration that one single computer can perform the effective data processing and signal control. The data acquisition system with one single computer has had a major influence on developing instrumentation and control software. For optical fiber pressure sensing system of this thesis, the tactile pressure is modulated by the voltage signal and processed by the computer. Finally, the system is flexible enough to have the ability to process signals from different sensors at the same time.

CHAPTER 6

ROBOT CONTROL AND MATRIX CONFIGURATION SENSORS

6.1 INTRODUCTION

As introduced in the abstract, this thesis presents potential applications of optical fibers as tactile pressure sensors. So far, the fiber sensor , the sensor system, and the computer interfacing have been discussed. In this chapter, the fiber tactile sensor is built on a robot hand to demonstrate the practical application of such a sensor. To lead to this discussion, section 6.2 will introduce the controlling of a robot arm with a fiber sensor on its hand. This robot system will perform the tactile sensing capability to monitor the magnitude of the contact pressure which is caused by grasping the object in the robot hand.

section 6.3 discusses the possible application of such fiber tactile sensor with a matrix configuration. This matrix configuration of the sensor system consists of several fibers in the system to build a two-dimensional planar sensing, and this configuration is proposed to be one superior method for the robot's tactile sensing capability.

6.2 ROBOT CONTROL

In this thesis, a MiniMover-5 robot arm manipulator (Micorbot, Inc.) is used to demonstrate the practical

application of the tactile fiber sensor. The MiniMover-5 manipulator is a five-jointed mechanical arm with a lifting capacity of 8 ounces when fully extended. Each joint is controlled by a stepper motor mounted on the body. In this demonstration, the fiber sensor is built on the hand. Also since we are concerned with the tactile pressure sensing, the stepper motor, which controls the hand, is the main consideration in both the driving circuit and the software programming.

The computer interfacing of the MiniMover-5 is designed so that an 8-bit computer can drive the 6 stepper motors of the robot arm by sharing the 8-bit parallel address buses and 8-bit parallel data buses with the use of an address decoder. As shown in Fig. 24, the structure of the MiniMover-5 computer interfacing, six stepper motor drivers and two input/output ports are addressed by the proper codes from the computer address buses. Then, as one of these eight drivers or ports has been addressed, the data on the data buses can be latched to the driving circuits. Notice that the low byte of the data buses (bit 0,1,2,3) is used for sending the sequential data for the stepper motors, and the high byte of the data buses (bit 4,5,6,7) is reserved for the auxiliary input port. The detail of the stepper motor operation and the driving codes is in Appendix B. Also, since the circuit has input/output ability, the sensor signals from the A/D converter can be sent into the computer by the auxiliary input port.

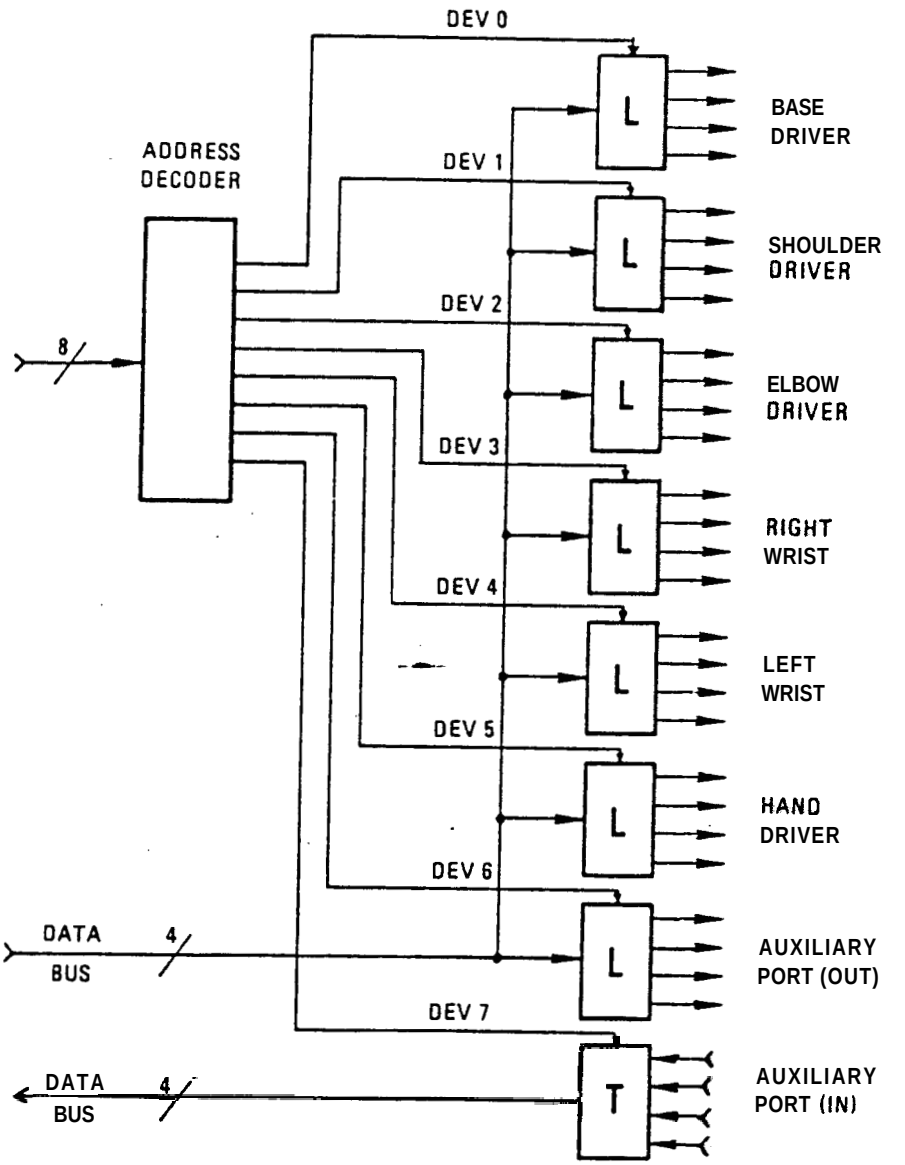

Fig. 24.--The MiniMover-5 computer interfacing.

The address decoding circuitry of the MinoMover-5 is shown in Appendix B. The address lines AO-A2 specifies which one of the eight decoder output will go low. As one of the outputs from the decoder is low, the OUT pulse is present. Then, a positive driving device selects pulse results. These pulses (DEV 0 to DEV 6) are used to latch data into one of the 6 motor driver circuitries. The tabulation of the addresses for the MiniMover-5 is given in Table 10.

TABLE 10

TABULATION OF THE ADDRESSES FOR THE MINIMOVER-5

Address		Port
Decimal	Binary	
152	10011000	Base Motor
153	10011001	Shoulder Motor
154	10011010	Elbow Motor
155	10011011	Wrist Right Motor
156	10011100	Wrist Left Motor
157	10011101	Hand Motor
158	10011110	Auxiliary Output
159	10011111	Auxiliary Input

For monitoring the magnitude of the tactile pressure from the A/D converter, one should build a table for the relationship between the input voltages and the output digital representations of the A/D converter in the program. For a 5V full scale A/D converter, its analog inputs vs digital outputs are shown in Appendix C. Since the magnitude of the pressure is already built in the program , the digital signals will be compared with the pressure-digital representation table in the program. Then, the magnitude of the applied pressure is decided by

the software.

A sample Basic program of controlling the MiniMover-5 with an optical fiber tactile pressure sensor is written as follows:

```
1  REM *** BEGIN ***
2  DATA 5,6,10,9
5  REM *** READ DATA ***
20 DIM A(8)
25 FOR 1=1 TO 8
30 READ A(I)
35 A(9-I)=A(I)
40 NEXT I
50 REM *** INPUT FROM KEYBOARD ***
510 A$=INKEY$:IF A$= " " THEN 510
520 NA=ASC(A$)
525 IF NA=53 THEN 1000
530 IF (NA>=49) AND (NA<=54) THEN 600
540 IF NA=9 THEN 560
550 IF NA=8 THEN 580
555 GOTO 510
560 REM *** DATA FOR MOTORS ***
561 FOR J=l TO 4: OUT I,A(J)
562 NEXT J
565 A$=INKEY$; IF A$= " " THEN 560
570 GOTO 510
580 FOR J+l TO 4: OUT I,A(J+4):NEXT J
585 A$=INKEY$:IF A$= " " THEN 580
590 GO TO 510
600 I=NA+103
610 PRINT "MOTOR";I-151;"READY "
620 GOTO 510
630 REM *** INPUT SENSOR SIGNALS ***
1000 IF NA=9 THEN 560
1010 IF NA=8 THEN 1020
1020 DATA 0,5,0
1030 DIM B(3)
1040 FOR 1=1 TO 3
1050 READ B(I)
1060 NEXT I
1070 REM *** START CONVERSION ***
1080 OUT 158, B(I)
1090 C=INP(159)
1100 IF C<=SETPOINT THEN 1600
1200 IF C>SETPOINT THEN 1300
1300 FOR J=l TO 4; OUT I, A(I)
1400 NEXT J
1500 GOTO 1070
1600 PRINT "SET POINT PRESSURE"
1700 GOTO 50
```

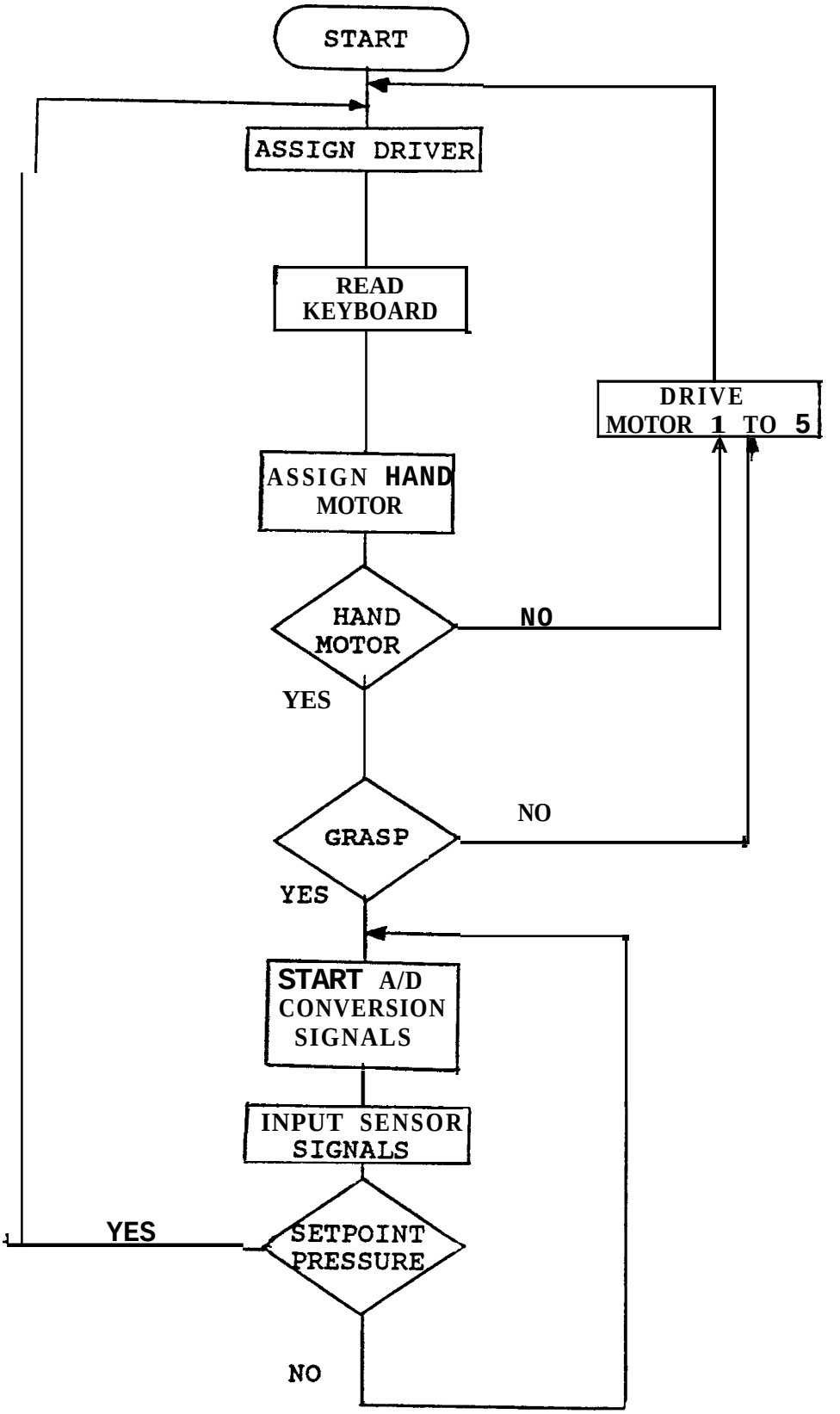

Fig. 25.--Flow chart of the basic program for MiniMover-5.

6.2 MATRIX ARRAY CONFIGURATION OF THE FIBER SENSOR

The robot with sensing capabilities will become much smarter than just a duplicate-machine. So far, the current robot system has a vision sensing capability or other types of relatively simple sensing devices. However, the development of tactile sensing for the robot has been researched to simulate human tactile capabilities. The robot with such a capability can handle sophisticated tasks more efficiently than those robots which are now used in industry. Although there are many tactile sensor configurations which have been used in developing such tactile sensing capability, matrix array configuration of the fiber sensor can be the one efficient method.

As discussed before, one single fiber sensor can detect the amount of pressure which is applied on the fiber. However, there is a big difference between simple touch sensing and tactile sensing. Tactile sensing involves continuous and variable measuring of the contact pressure. In other words, tactile sensors should have the capabilities to report graded signals and parallel patterns of touching. In an advanced robot system, the robot should have the two dimensional tactile sensing capability which is proposed in this section.

Consider the matrix configuration of the fiber sensor in Fig. 26., the fibers are constructed as a tennis racket structure. With eight light sources (T1 to T8) and

eight photodetectors (D1 to D8) in the area A, the system consists of a 4 by 4 matrix configuration which has sixteen intersection points (S1 to S16).

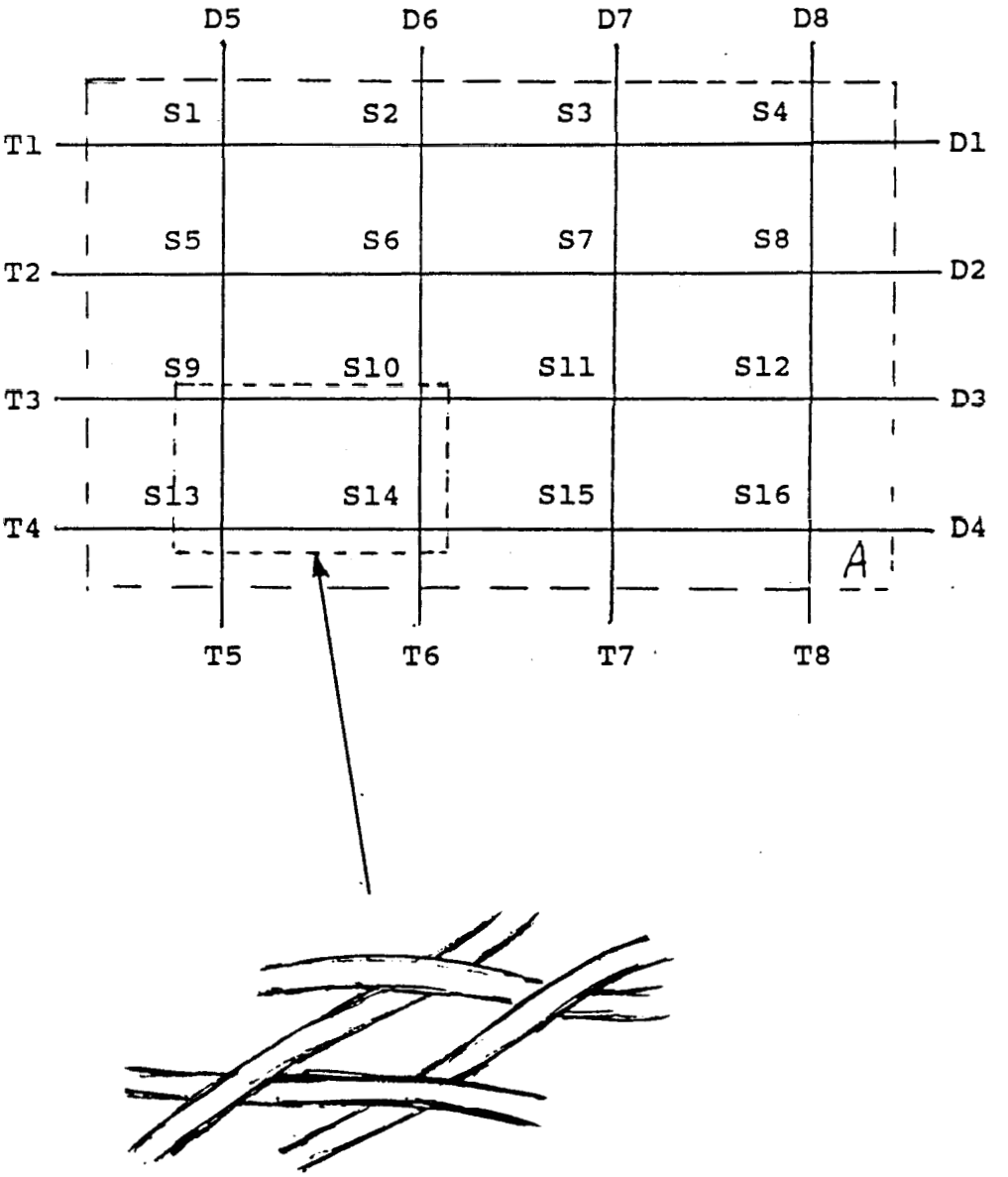

Fig. 26.--Matrix array configuration of the fiber sensors.

As pressure is applied to area A, photodetectors can monitor the pressure changes on these intersection points. For example, if the pressure is applied on S1 point only, then output voltages of the photodetectors D1 and D5 will respond to the pressure changes. By using this method, one can know the pressure location over the area A. As a graded pressure is applied to the area A, each two photodetectors will respond to the pressure on one S point. With the help of a digital computer's high speed scanning skills which were discussed in Chapter 5, the output voltages from these photodetectors can be sent into the computer and then be analyzed by the software programming. Thus, a two-dimension fiber sensor can be constructed which can be a superior method for robot's tactile sensing.

The advantages of matrix configuration sensor are the same as single fiber sensor such as small size, low cost, and electromagnetic noise immunity, etc. However, by using small radius glass fibers in the system, one should not be surprised by how small the sensor size can be built.

For analyzing the matrix array configuration of the fiber sensor, the state-space approach of the control theory is used in this section. Also, some assumptions are required to simplify the approach. First of all, the system is assumed to be time-invariant. In other words, the inputs, the outputs, and the state variables of the system are independent of the time change. Secondly, it is assumed that there are no exogenous inputs present in the system. Then we

are concerned only with the linear range of operation. Finally, it is assumed that there is no direct connection between the input and the output without the intervention of the state variable. In state-space method, a linear dynamic system is represented by equations:

$$Y = CX + DU \tag{26}$$

$$\dot{X} = AX + BU + EX, \tag{27}$$

where Y is the output vector,

X is the state variable vector,

U is the input vector,

and A,B,C,D,E are transfer matrices of the system.

According to the assumptions of the system, D matrix is assumed equal to zero because there is no direct relation between input and output without the intervention of X. Also, since there is no exogenous input, X_0 is equal to zero. Then, Eq. (26) and Eq. (27) become:

$$Y = CX \tag{28}$$

$$\dot{X} = AX + BU. \tag{29}$$

In the matrix array fiber sensor system, the applied pressure changes (ΔP) are defined as the state variables, and the output voltage changes (ΔVa) are defined as outputs of the system. Since a 4x4 matrix has sixteen intersection points and each two photodetectors decide one output of the system, then the Eq. (28) becomes:

$$Y = \begin{bmatrix} Val \\ Va2 \\ \\ \\ \\ Va16 \end{bmatrix} - [C1, C2 \ldots\ldots, C16] \begin{bmatrix} P1 \\ P2 \\ . \\ . \\ . \\ . \\ . \\ P16 \end{bmatrix} \qquad (30)$$

where C matrix is the transfer function of the state variable and output. If the configuration of the fibers in this system is constructed symmetrically, all sixteen elements of the C matrix will be identical, i.e. C1=C2=.....=C16. Notice that each element of the output vector is combined by two photodetectors' voltage changes. For example, the output Val is the combination of the voltage changes of D5 and D1 in Fig. 26.

To derive the state equation, one can analyze the stress, pressure relation on the fiber, and derive the transfer function A and C. However, this thesis is concerned mainly with the sensor system , and the control theory of the system is left for further study.

6.4 SUMMARY

In this Chapter, the robot control and matrix configuration sensors are discussed. In Appendix D, the actual robot control which was built with a spiral fiber sensor is demonstrated. In addition, the assembler program of the robot control and the analysis of the system are listed.

CHAPTER 7

CONCLUSION

The objective of this thesis is to examine potential applications of optical fiber pressure sensors, and to provide a tactile pressure measurement method which is then used in a robot system. Modeling, measurement, analysis, and application of the fiber pressure sensor are presented.

The intrinsic type of fiber sensor used for tactile pressure sensing is discussed in Chapter 2. This type of sensor utilizes the microbending of the fiber to modulate the applied pressure on the fiber. The light loss in the core of the fiber is sensitive to the curvature of the fiber.

To model and develop a mathematical representation for the fiber pressure sensor, the waveguide ray approach is used. Chapter 3 derives the power attenuation equation due to the leaky rays of the fiber. The radiation loss due to these leaky rays, either by refracting or tunneling, are then described by the ray invariants of the ray approach.

Depending on the design of the sensor structure, different structures will have different responses to the applied pressure on the fiber. The experimental results in Chapter 4 indicate that the sensitivity of the sensor is related to:

(1) The diameter of the fiber.

(2) the number of bendings on the fiber.

(3) The surface area of the applied pressure.

(4) The material properties of the fiber.

(5) The structure of the sensor design.

The experimental results also indicate that the sensor designs to achieve fiber distortions are effective to measure the tactile pressure.

Computer-controlled sensor systems can perform effective data acquisition processing and signal control. These computer-controlled sensor systems are discussed in Chapter 5. This tactile sensor system was built and tested in order to demonstrate the feasibility of the system. The results of this demonstration is described in Chapter 6.

For further investigation, a matrix array configuration of the fiber sensor could be considered to provide the robot system a two-dimensional plannar tactile-pressure sensing. Such fiber tactile pressure sensor could be used in many engineering applications depending upon the development engineer's imagination.

APPENDIX A

Description of KOP–100

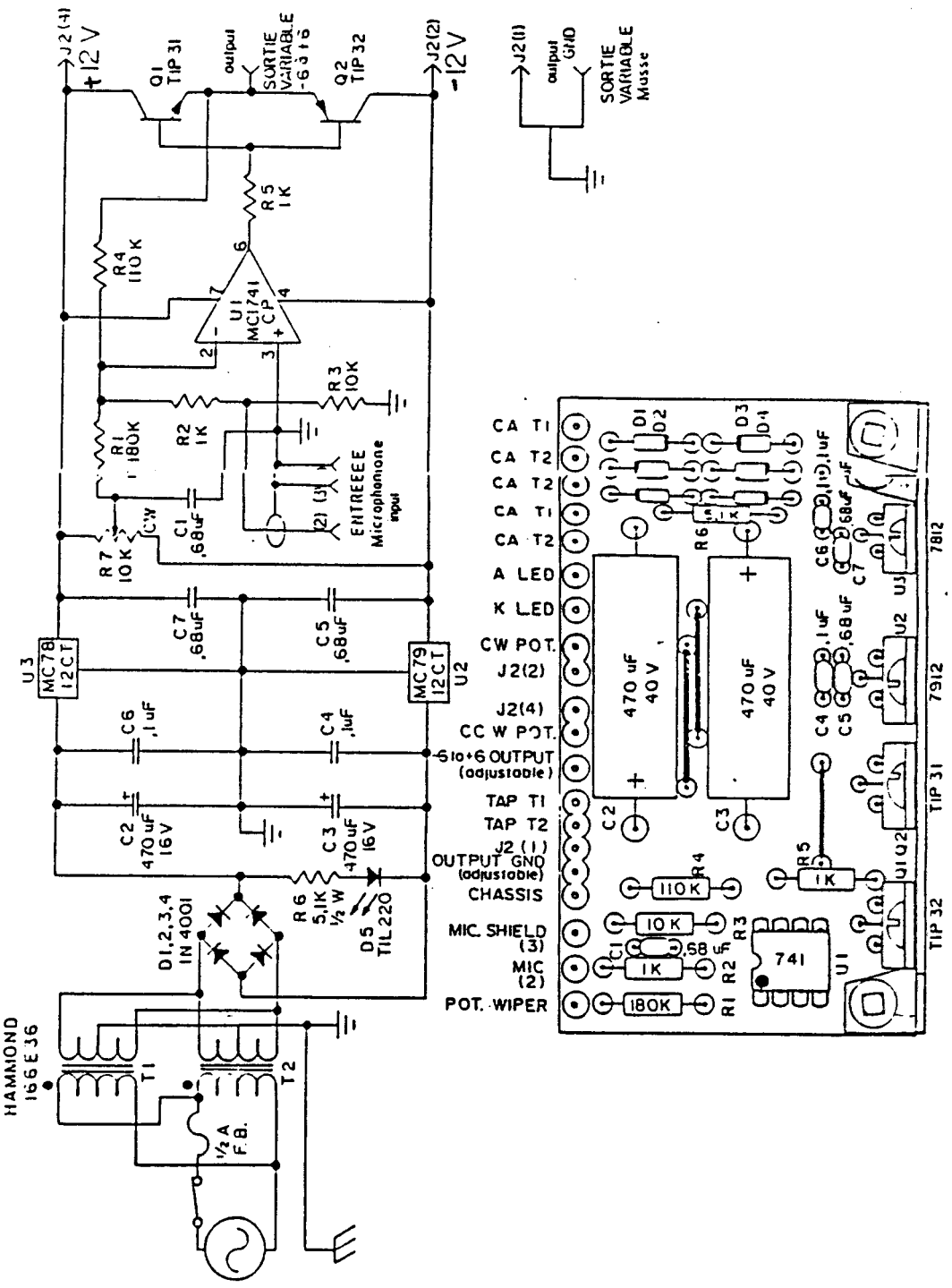
+12 V
-12 V
Q1 TIP 31
Q2 TIP 32
output
SORTIE VARIABLE -6 à +6
R4 110 K
R5 1K
U1 MC1741 CP
R3 10K
R2 1K
R1 180K
R7 10K
CW
C1 .68uF
ENTREEEE Microphonique input
C7 .68uF
C5 .68uF
U3 MC78 12CT
MC79 12CT U2
C6 .1uF
C4 .1uF
C2 470 uF 16V
C3 470 uF 16V
R6 5.1K ½ W
D5 TIL 220
D1,2,3,4 IN 4001
HAMMOND 166E36
T1
T2
½ A F.B.
J2(1)
output GND
SORTIE VARIABLE Musse
CA T1
CA T2
CA T2
CA T1
CA T2
A LED
K LED
CW POT.
J2(2)
J2(4)
CC W POT.
-6 to +6 OUTPUT (adjustable)
TAP T1
TAP T2
J2(1)
OUTPUT GND (adjustable)
CHASSIS
MIC. SHIELD (3)
MIC (2)
POT. WIPER
D1 D2 D3 D4
470 uF 40 V
110K
10 K
1K
180K
.68
741
7812
7912
TIP 31
TIP 32

COMPONENTS CHARACTERISTICS

FIBER

Plastic core and cladding
Step index type
Outside diameter: 1.52 mm (0.060 in)
Core diameter: 1.42 rnm (0.056 in)
Numerical aperture: 0.48
Attenuation: 1000 dB/km at 650 n m

TIL 24 LED (12)

Emitting wavelength: 940 n m
Spectral bandwidth: 50 n m
Half-power angle ($\theta_{\frac{1}{2}}$): 35"
Output flux at 50 mA: 7 mW/Sr

TIL 221 LED (13)

Internal resistor: 39 Ω
Maximum current: 50 mA
Maximum voltage: 4 V
Wavelength: 650 n m

TIL 99 PHOTOTRANSISTOR (15)

a- Phototransistor configuration (fig. 1)
- photocurrent: 5 mA for 20 mW/cm^2 from a 2870" K source
- risetirne t_r (fig. A2.1b): 8 μs
- falltime t_f: 6 μs

b) Photodiode configuration (fig. 2)
- photocurrent: 40 μA for 20 mW/cm^2 from a 2870" K source
- risetirne: 350 ns
- fall time: 500 ns

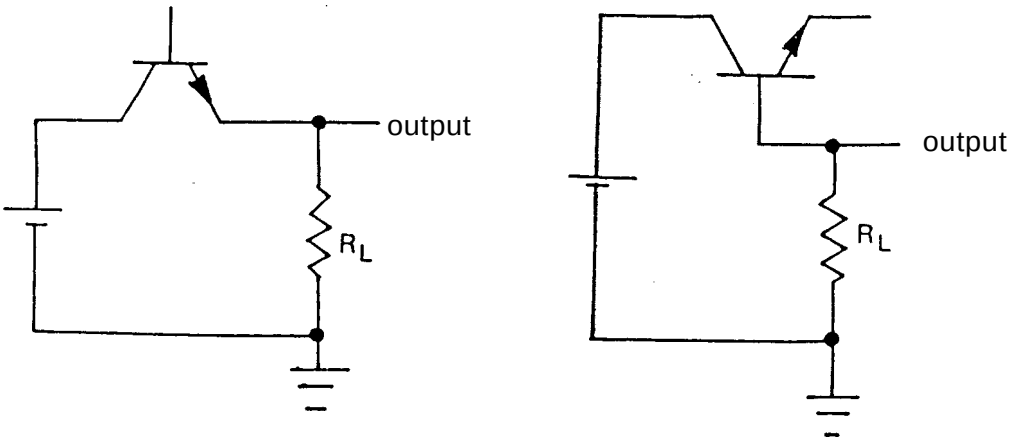

C 30808 PIN **PHOTODIODE** (14)

Type: RCA **C30808**
Photosensitive surface: 5mm^2
Spectral response (10%) 400 to 1100 nm
Peak inverse voltage: 100 V
Photocurrent density: 5 mAlmm^2 DC
20 rnA/mrn^2 peak
Forward current (I_f): 10 **mA** DC
100 **mA** peak
Dark current: 30 **nA**
Sensitivity at 900 nrn: 0,6 **A/W**
at 1060 nm: **0,15 A/W**
Quantum efficiency at 900 nm: **80%**
at 1060 nm : **17%**
Equivalent noise power: at 900 nrn: 1.5 **x 10^{-13} W/Hz$^{\frac{1}{2}}$**
(at 1000 Hz, Af = 1 Hz) at 1060 nm: 6.5 **x 10^{-13} W/Hz$^{\frac{1}{2}}$**
Risetime: at **900 nm** : 5 ns
(with reverse bias) at 1060 nm : 8 ns

PARTS LIST

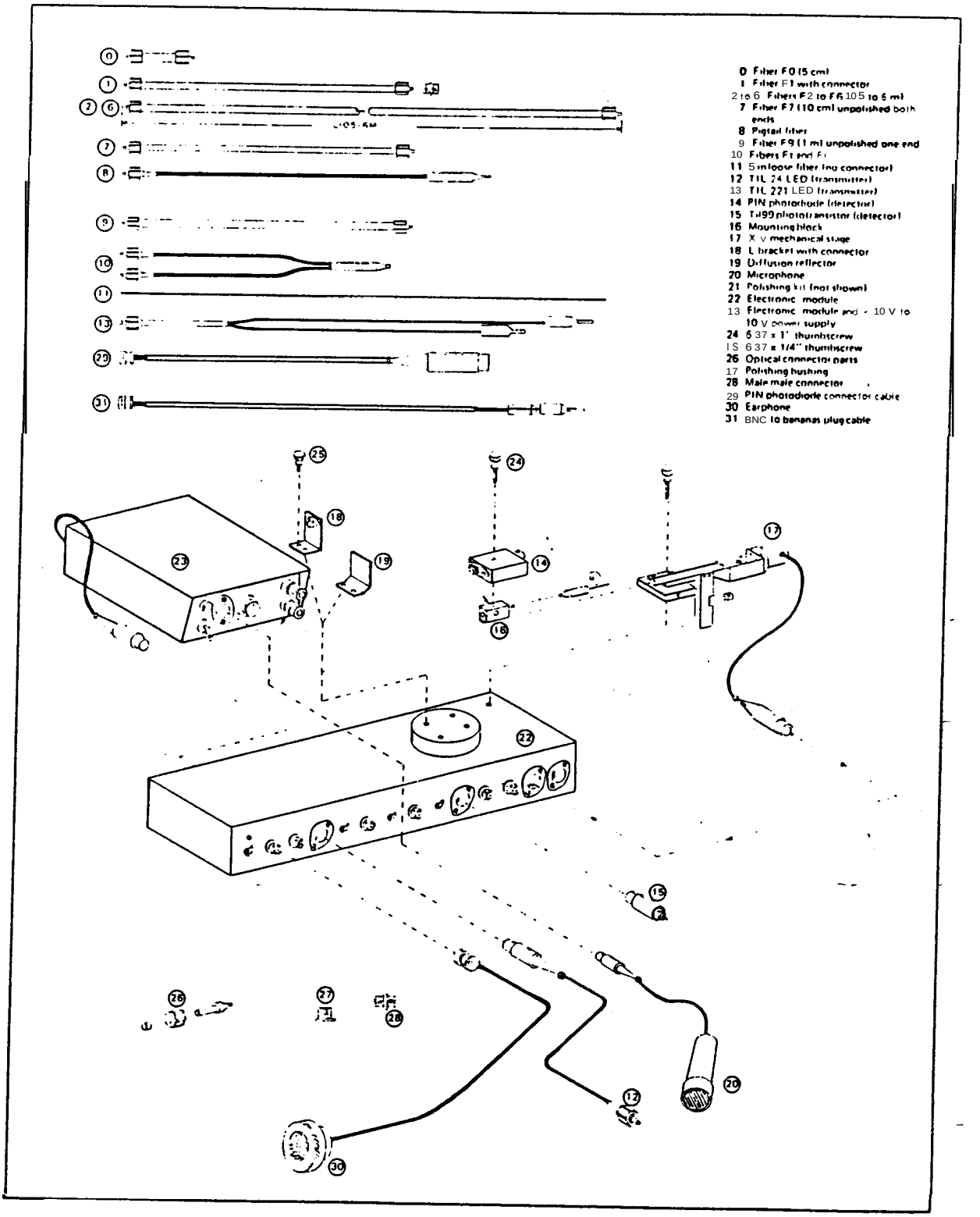

0 Fiber F0 (5 cm)
1 Fiber F1 with connector
2 to 6 Fibers F2 to F6 105 to 6 m)
7 Fiber F7 (10 cm) unpolished both ends
8 Pigtail fiber
9 Fiber F9 (1 m) unpolished one end
10 Fibers F4 and F5
11 5 m loose fiber (no connector)
12 TIL 24 LED (transmitter)
13 TIL 221 LED (transmitter)
14 PIN photodiode (detector)
15 TIL99 phototransistor (detector)
16 Mounting block
17 X Y mechanical stage
18 L bracket with connector
19 Diffusion reflector
20 Microphone
21 Polishing kit (not shown)
22 Electronic module
13 Electronic module and + 10 V to **10** V power supply
24 6 37 x 1" thumbscrew
15 6 37 x 1/4" thumbscrew
26 Optical connector parts
17 Polishing bushing
28 Male male connector
29 PIN photodiode connector cable
30 Earphone
31 BNC to bananas plug cable

APPENDIX B

STEPPER MOTOR AND MINIMOVER-5

STEPPER MOTOR

The stepper motors of the **MiniMover-5** use 4 coils structure, and each coil is driven by a power transistor. With the transistors either turned on or turned off to obtain the desired pattern of currents in the motor windings, the computer drives the motor. By changing the pattern of currents, a rotating magnetic field is obtained inside the motor. This causes the motor to rotate in small increments or steps. In the Minimover-5, each of the four coils in a motor is individually controlled from the computer. The schematic diagram and the binary phase patterns of stepper motor are shown as follows:

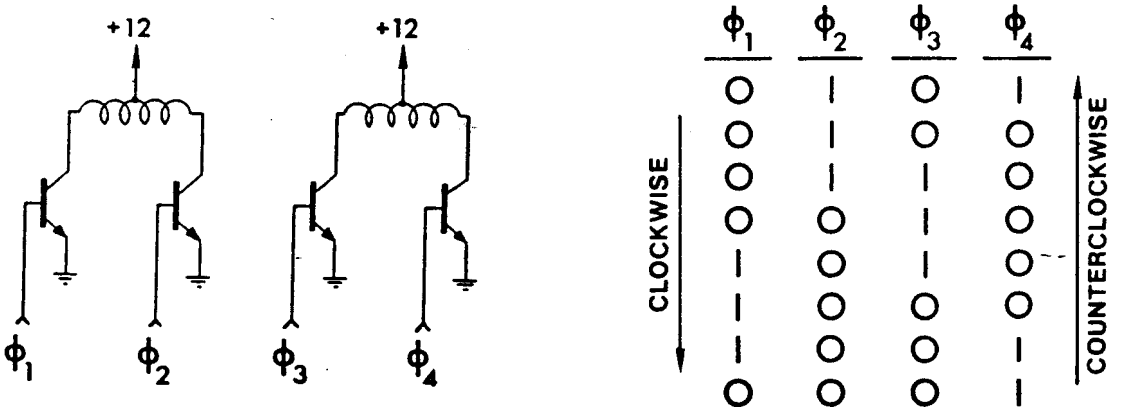

Fig. 27.--Binary phase patterns of stepper motor.

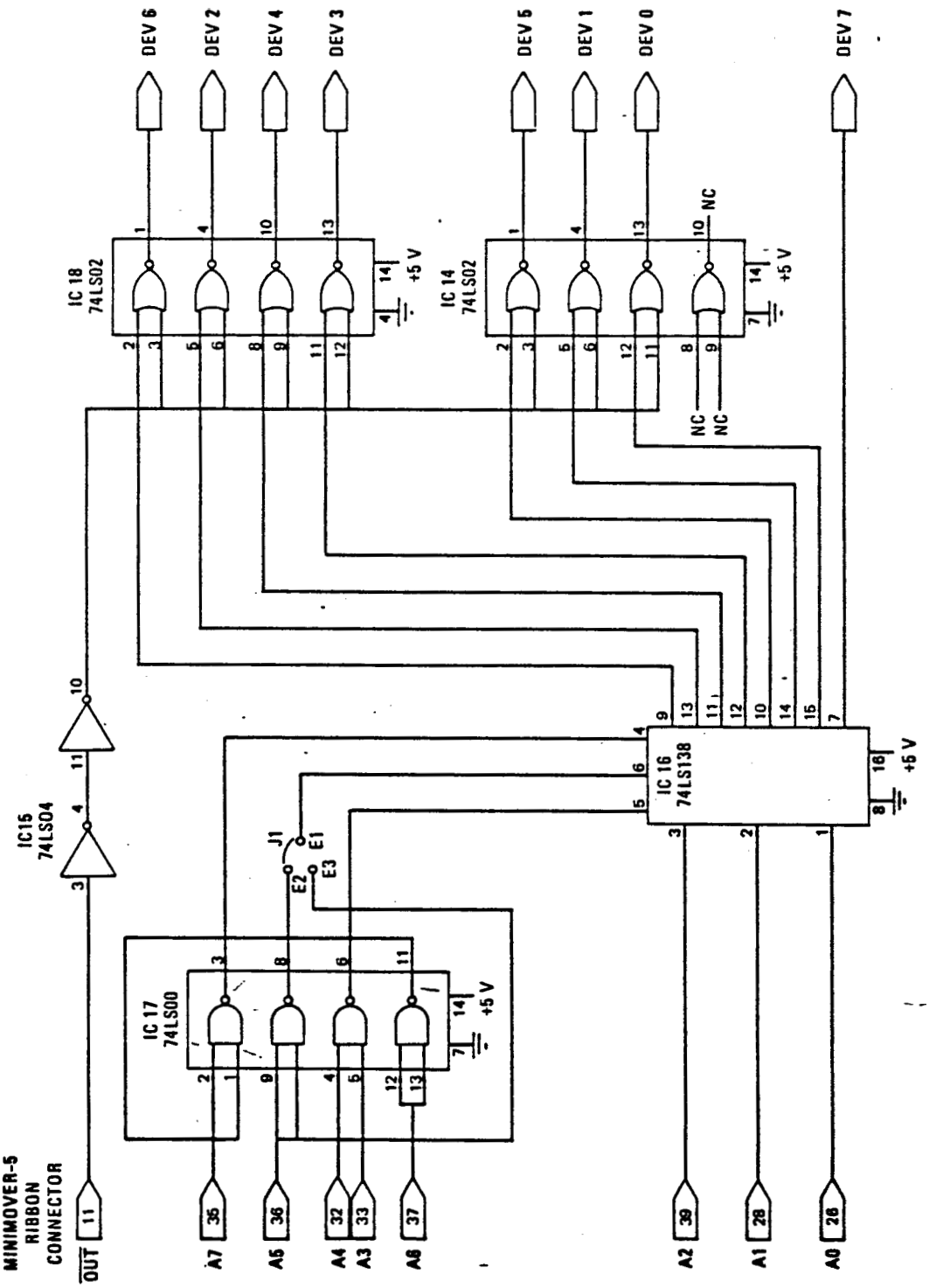

Fig. 28.--Address decoding schmatic.

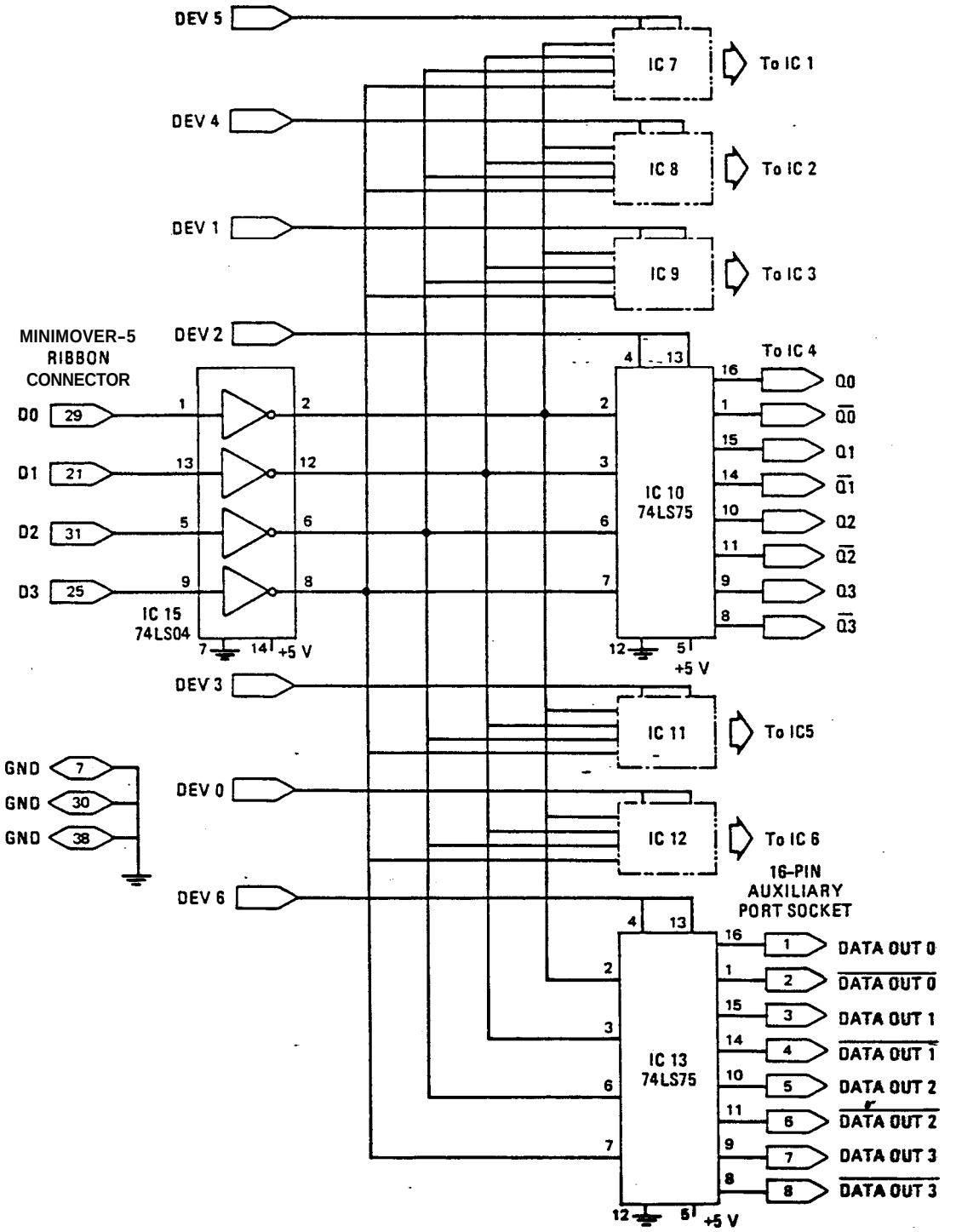

Fig. 29.--Output latching circuitry.

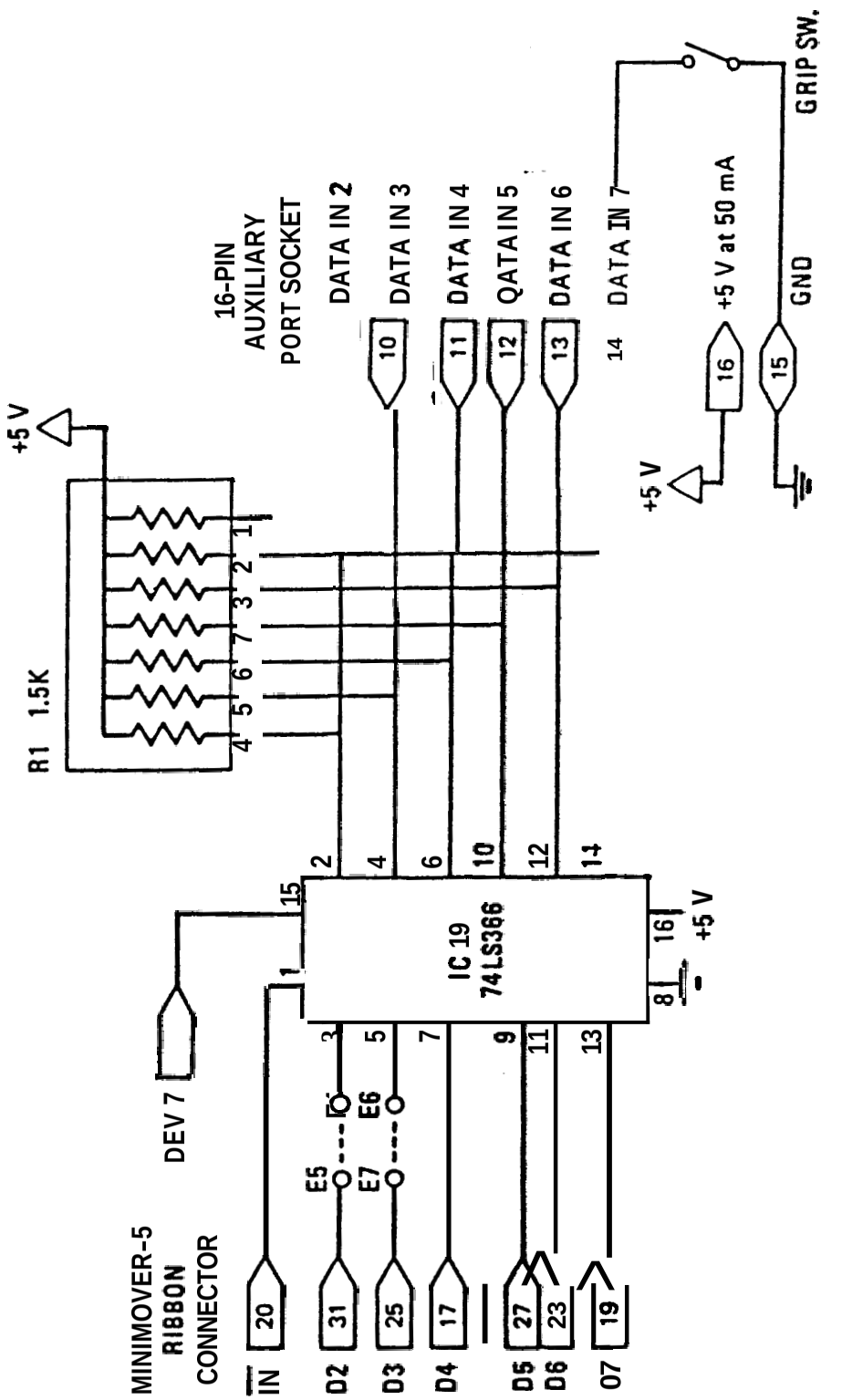

Fig. 30.--Input port circuitry.

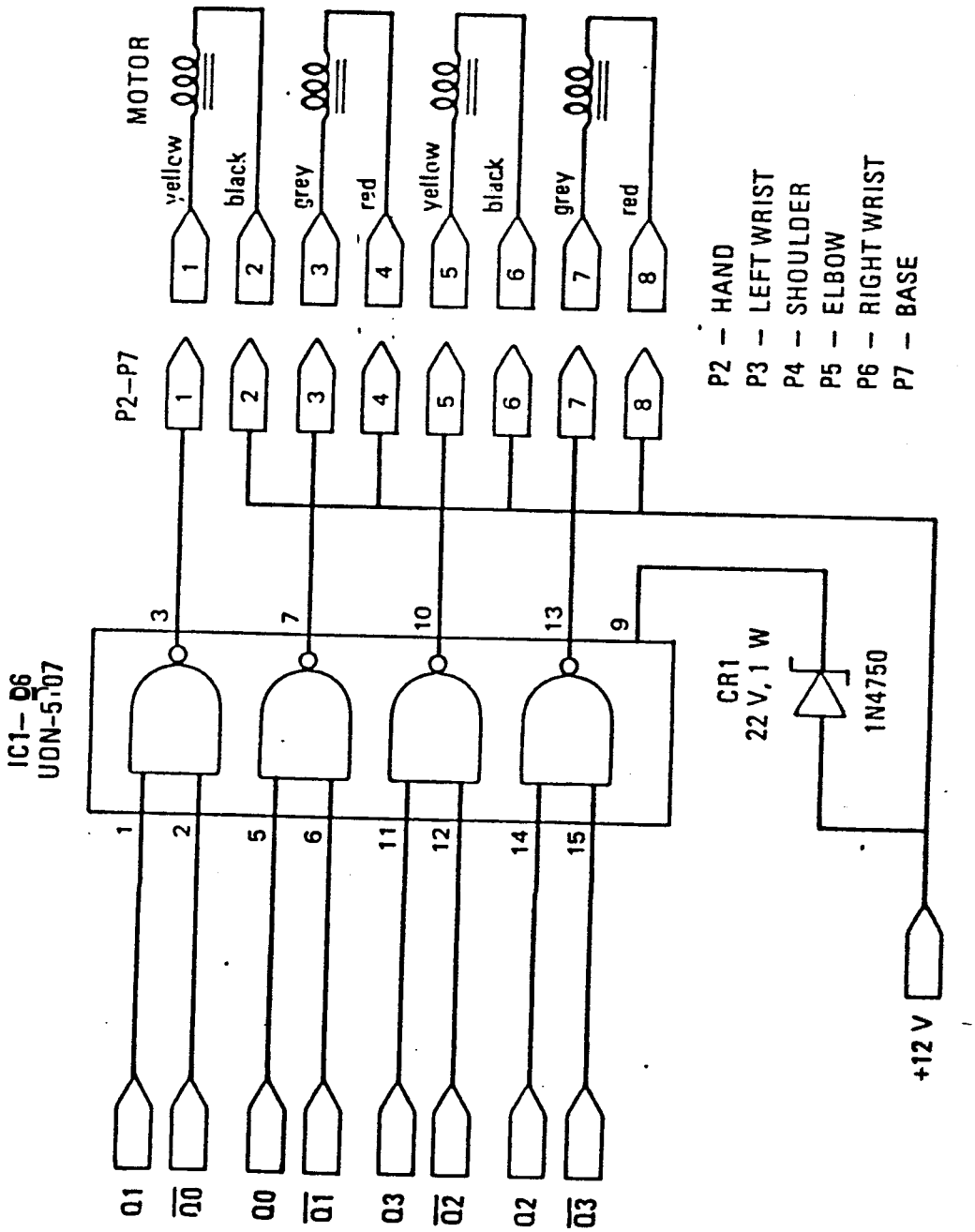

Fig. 31.--Stepper motor driver schematic.

APPENDIX C

DIGITAL OUTPUT CODES OF ADC0808

TABLE 11

DIGITAL OUTPUT CODES OF ADC0808

ANALOG INPUT VOLTAGE	DIGITAL OUTPUT CODES
5v	1 1 1 1 1 1 1 1
2.5V	1 0 0 0 0 0 0 0
1.25V	0 1 0 0 0 0 0 0
0.625V	0 0 1 0 0 0 0 0
0.3126V	0 0 0 1 0 0 0 0
0.156V	0 0 0 0 1 0 0 0
0.078V	0 0 0 0 0 1 0 0
0.039V	0 0 0 0 0 0 1 0
0.0195V	0 0 0 0 0 0 0 1
0V	0 0 0 0 0 0 0 0

APPENDIX D

ASSEMBLER PROGRAM AND ANALYSIS OF THE SYSTEM

The control program of the MiniMover-5 with an spiral fiber sensor by an INTEL-SDK85 is written as follows:

```
     SOURCE STATEMENT                COMMENT

2000           LXI SP 20C2           BEGIN
               MOV A,08
               SIM
2006 BEGIN:    CALL RDKBD            ASSIGN MOTOR
               MOV B,A
               CALL UPDDT
               INR B
               MOV A, B
               OUT 21                ASSIGN OUTPUT PORT
               CPI 00                MOTOR 0
               JZ TURN
               CPI 01                MOTOR 1
               JZ TURN
               CPI 02                MOTOR 2
               JZ TURN
               CPI 03                MOTOR 3
               JZ TURN
               CPI 04                MOTOR 4
               JZ TURN
               CPI 05                MOTOR 5
               JZ TURN
               JMP BEGIN             WAIT TILL MOTOR IS
                                        *ASSIGNED
2032 TURN:     MVI A, OF
               OUT 20                ASSIGN OUTPUT PORT
               MOV A, B
               OUT 21                OUTPUT MOTOR ADDRESS
2039 LOOPO:    CALL RDKBD            ASSIGN DIRECTION
               MOV B,A
               CALL UPDDT
               INR B
               MOV A, B
               CPI OF
               JZ RLOOP              RIGHT TURN
               CPI OE
               JZ LLOOP              LEFT TURN
               JMP LOOPO             WAIT
204F RLLOP:    MVI A, 05             RIGHT TURN DRIVING
               CALL OUTLOOP          OUTPUT PATTERNS AND
               MVI A, 06                *TIME DELAY
               CALL OUTLOOP
               MVI A, OA
               CALL OUTLOOP
               MVI A, 09
               CALL OUTLOOP
```

	SOURCE STATEMENT	COMMENT
	MVI A, 00	ASSIGN INPUT PORT
	IN 01	SWITCH PORT
	CPI 00	STOP DRIVING?
	JZ BEGIN	STOP
	JMP **RLOOP**	
2071 **LLOOP:**	MVI A, 01	LEFT TURN DRIVING
	CALL **OUTLOOP**	OUTPUT PATTERNS AND
	MVI A, 09	*TIME DELAY
	CALL **OUTLOOP**	
	MVI A, 08	
	CALL **OUTLOOP**	
	MVI A, OA	
	CALL **OUTLOOP**	
	MVI A, ***02***	
	CALL **OUTLOOP**	
	MVI A, 06	
	CALL **OUTLOOP**	
	MVI A, 04	
	CALL **OUTLOOP**	
	MVI A, 05	
	CALL **OUTLOOP**	
	MVI A, ***00***	ASSIGN INPUT PORT
	OUT 02	*FOR SENSOR SIGNAL
	IN 01	
	CPI 00	STOP DRIVING ?
	JZ BEGIN	
	IN 00	INPUT SENSOR SIGNAL
	CPI SETPOINT	COMPARE WITH **SETPINT**
	JM BEGIN	SMALLER THAN **SETPOINT**
	JMP LLOOP	DRIVING
20B0 OUTLOOP:	OUT ***22***	
	LXI **D,05,05**	MOTOR SPEED
	CALL DELAY	
	RET	

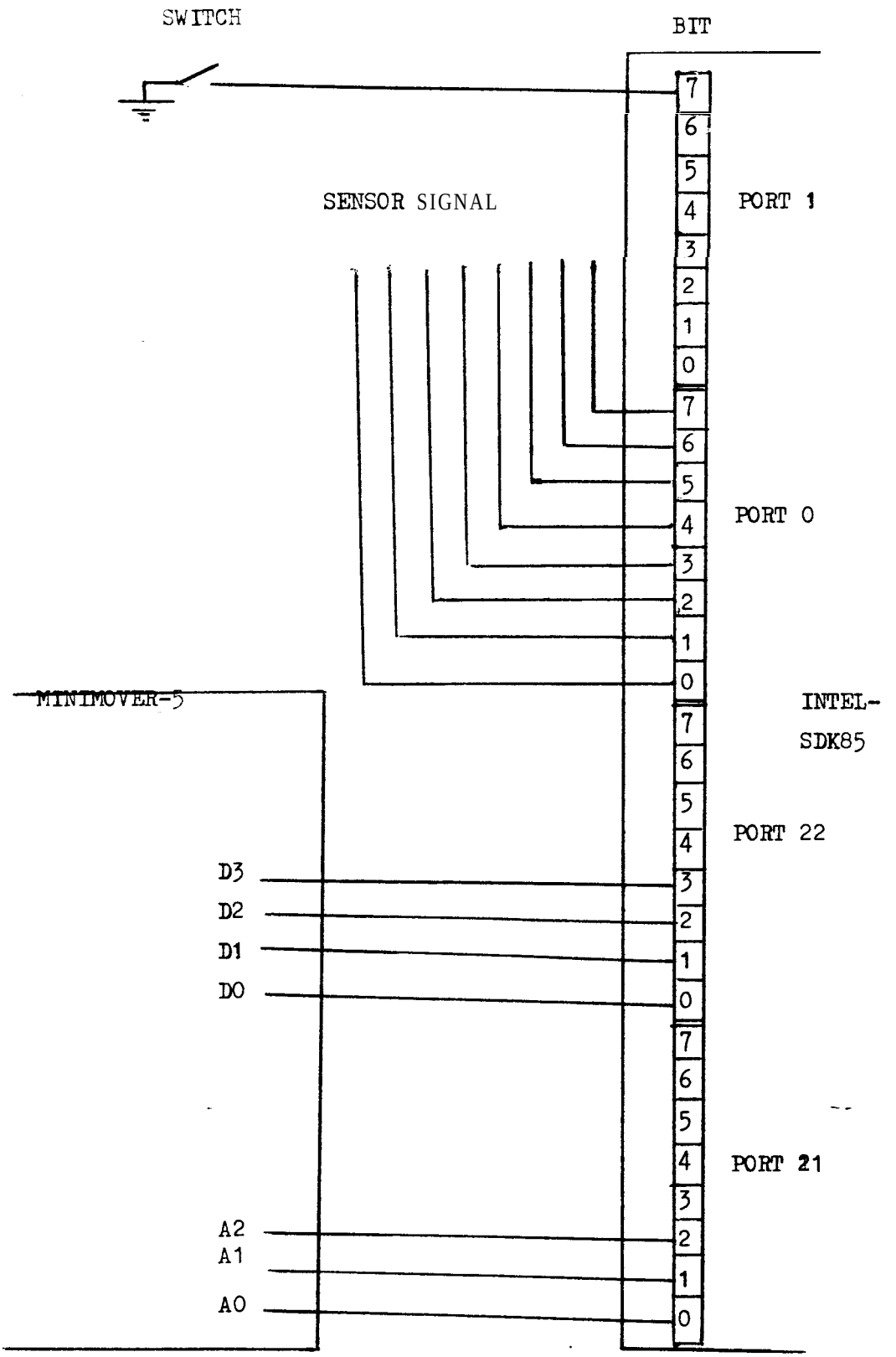

Fig. 32.--Interfacing circuitry of the system.

Errors in the sensor system occur due to:

(1) the delay in the computer generated signal to stop the motor after the set point pressure is reached,

(2) the instability of the light signal, and

(3) the mechanical vibrations of the robot.

There are two ways to reduce these errors:

(1) reduce the speed of the motor while the robot is grasping the object, and

(2) use electronic circuitry to anticipate the errors and correct them with software programing.

The sensitivity of the sensor is determined by the following factors:

(1) Sensor design.

(2) Motor speed.

(3) Set point of the program.

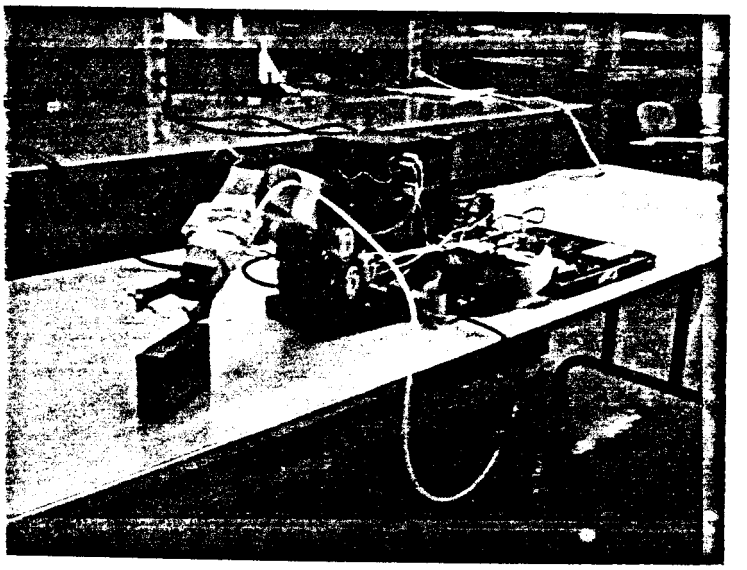

Fig. **33.--Set up of the sensor system.**

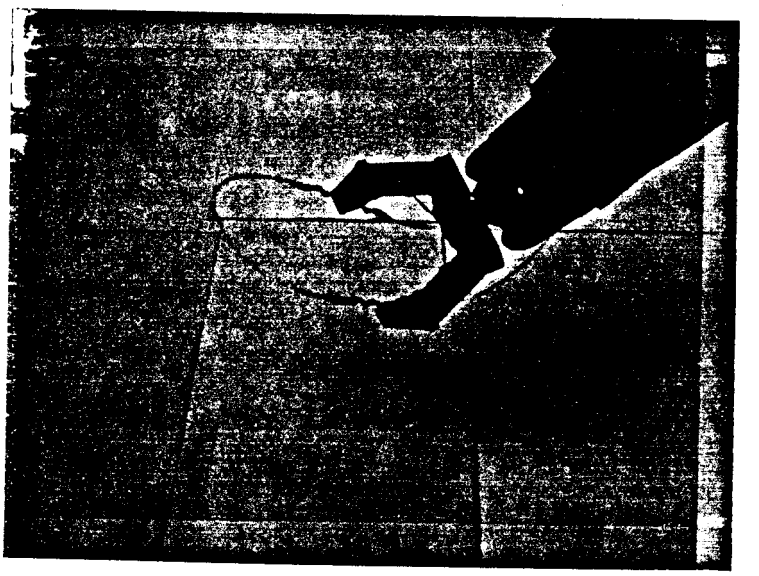

Fig. **34.--A spiral fiber sensor on the robot hand.**

BIBLIOGRAHPY

Books

Barney, George C., Intelligent Instrumentation, Prentice-Hall, Inc., 1985

Cheo, Peter K., Fiber Optics Devices and Systems, Prentice-Hall, Inc., 1985.

Dally, James W. and McConnell Kenneth G., Instrumentation For Engineering Measurements, Wiley, 1984.

Hordeski, Michael F., Design of Microprocessor Sensor & Control Systems, Reston Publishing Company, Inc., 1985.

Keiser, Gerd., Optical Fiber Communications, Chapman and Hall, Inc., 1983

Snyder, Allen W. and Love, John D., Optical Waveguide Theory, Chapmen and Hall, 1983.

Wist, Aboud O. and Meikson, Z. H., Electronic Design of Microprocessor Based Instruments and Control Systems. Prentice-Hall, Inc., 1986.

Articles

Bak, David J. "Optic Fiber Senses Pressure.", Design News, 3, March 1986.

Dandridge, A., "Fiber Optic Sensors." CEP. , January 1986.

Das Santanu, Collin G. Englefield, and Paul A. Goud, "Power Loaa, Modal Noise and Distortion Due to Micorbending of Optical Fibers.", Applied Optics.1, August 1985, Vol. 24.

Giallorenzi, Thomas G. and Bucaro, Joseph A., "Optical Fiber Sensor Technology.", IEEE Quantum Electronics.,4, April 1982, Vol. 18.

Marvin, Dean C. and Ives, Neil A., "Wide-range Fiber-optics Strain Sensor.", Applied Optics., 1, December 1984, Vol. 23.

Stafffer, Robert N.,"Progress in Tactile Sensor Development.", Robotics Today., June, 1983.

REFERENCES

Books

Barnoski, Michael K., Fundamentals of Optical Fiber Communications., Academic Press, Inc., 1976.

Cherin, Allen H., Introduction to optical Fibers., McGraw-Hill Book Company, 1983.

Friedland, Bernard, Control System Design., McGraw-Hill Book Comapny, 1986.

Norton, Hary N., Sensor and Analyzer Handbook., Prentice Hall, Inc, 1982.

Seippel, Robert G., Transducers, Sensors, and Detectors., Reston Publishing, Inc., 1983.

Articles

Ady Arie, and Moshe Tur, "Measurement and Analysis of Light Transmission through a Modified Cladding Optical Fiber with Applications to Sensors.",Applied Optics. 1, Jane 1986, Vol. 25.

McMahon, Donald H., "Fiber-optic Transducers.", IEEE Spectrum., Dec 1981.

Rourke, Michael D., "Measurement of the Insertion Loss of a Single Microbend.", Optical Society of America., Sept. 1981, Vol.6.

Tetsuji Abe, "Strain Sensor Using Twisted Optical Fibers.", Optical Society of America., August 1984, Vol. 9.